

INTRODUCTION IN OFFSHORE HYDROMECHANICS (OT3600)

First Edition



J.M.J. Journée and W.W. Massie

Delft University of Technology

March 2001

REPORT 1267-K

Contents

1	Introduction	1
2	Static Floating Stability	2
3	Resistance and Propulsion	10
3.1	Scaling	10
3.2	Resistance	12
3.3	Propulsion	14
3.4	Propulsion versus Resistance	22
4	Summary of Ocean Surface Waves	23
4.1	Regular Waves	23
4.2	Irregular Waves	25
5	Behavior of Structures in Waves	35
5.1	Behavior in Regular Waves	35
5.1.1	Equations of Motion	37
5.1.2	Frequency Characteristics	43
5.2	Behavior in Irregular Waves	46
5.2.1	First Order Motions	46
5.2.2	Second Order Motions	49

Chapter 1

Introduction

These lecture notes present a short introduction in offshore hydromechanics on behalf of the lectures OT3600 and OT3610 for offshore technology students.

Use has been made here of relevant parts of the Lecture Notes OT4620 on this subject:

OFFSHORE HYDROMECHANICS

(Preliminary Edition)

by: J.M.J. Journée and W.W. Massie

Delft University of Technology

August 1998

For more detailed information on offshore hydromechanics the reader is referred to these extensive notes; reference [Journée and Massie, 1998].

Chapter 2

Static Floating Stability

The static stability of a floating structure encompasses the up-righting properties of the structure when it is brought out of equilibrium or balance by a disturbance in the form of a force and/or a moment. As a result of these (extra) loads, the structure will translate and/or rotate about its center of gravity. Formally, dynamic as well as static properties of the structure play a role in this, but only the static properties of the structure will be considered here.

Definitions

The body axes and the notations, as used here in static stability calculations, are presented in figure 2.1.

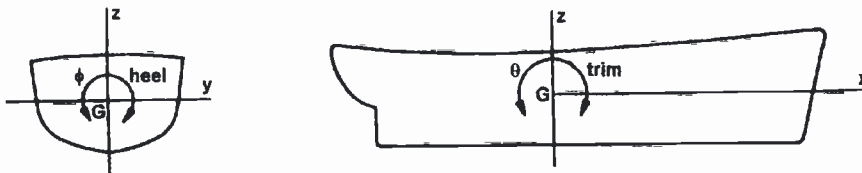


Figure 2.1: Body Axes and Notations

So-called hydrostatic forces and moments, caused by the surrounding water, will act on a structure in still water. The buoyancy of a structure immersed in a fluid is the vertical upthrust that the structure experiences due to the displacement of the fluid. The center of the volume of the fluid displaced by a floating structure is known as the **center of buoyancy** B , see figure 2.2-a. The **center of gravity**, G of a structure is that point through which, for static considerations, the whole weight of the structure may be assumed to act, see figure 2.2-b.

Rotations in the plane of drawing are defined here as heel, a rotation about the structure's longitudinal horizontal axis. The same principles holds as well for trim, a rotation about the body's transverse horizontal axis. Superposition can be used for combinations of heel and trim - at least if the angles of rotation are not too large.

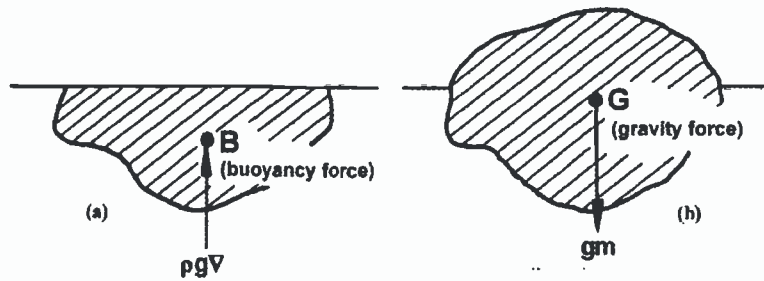


Figure 2.2: Definition of Centers and Forces

Vertical Equilibrium

For a floating structure, a vertical downward movement (sinking deeper) results in an increase of the buoyant force which will tend to force the structure back upwards; it tends to return the structure to its original state of balance so that the structure is stable for this type of disturbance.

Archimedes' principle holds for the vertical equilibrium between buoyancy and gravity forces:

$$\rho g \nabla = gm \quad (2.1)$$

where ρ is the mass density of the fluid, g is the acceleration of gravity, ∇ (nabla) is the volume of the submerged part of the structure and m is the mass of the structure. For sea water, the mass density, ρ , is in the order of 1025 kg/m^3 .

If an additional mass, p , is placed on this structure, its original equilibrium will be disturbed. The structure will sink deeper and heel until a new state of balance has been reached. The new vertical balance is given by:

$$\rho g \cdot (\nabla + \Delta \nabla) = g \cdot (m + p) \quad (2.2)$$

in which $\Delta \nabla$ is the increase of the volume of displacement of the floating structure.

If the mass p has been placed on the structure in such a manner that it only sinks deeper parallel to the water plane without heel, the change of draft ΔT follows from:

$$\Delta \nabla = \Delta T \cdot A_{WL} = \frac{p}{\rho} \quad \text{or:} \quad \Delta T = \frac{p}{\rho \cdot A_{WL}} \quad (2.3)$$

Here, A_{WL} is the area of the water plane. It is implicitly assumed that this area is constant over the draft interval ΔT , by the way.

Rotational Equilibrium

If an external heeling moment acts on the structure as given in figure 2.3, it follows from the rotational balance:

$$M_H = \rho g \nabla \cdot y = gm \cdot y \quad (2.4)$$

From this follows too that if no external moment acts on the structure, the lever arm y should be zero:

$$M_H = 0 \quad \text{results in:} \quad y = 0 \quad (2.5)$$

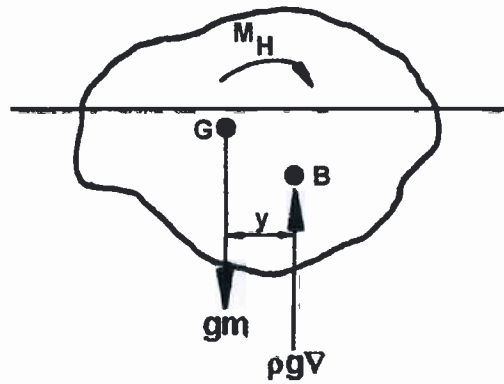


Figure 2.3: Heeling Moment

This means that for any floating structure at rest, the center of buoyancy B and the center of gravity G will be situated on the same vertical line. If this is not so, the structure will heel or trim until they do become vertically aligned. This means too that the longitudinal position of the center of gravity can be found easily from the longitudinal position of the center of buoyancy, which can be derived from the under water geometry of the structure.

Shifting Masses and Volumes

Consider a structure with a mass m . This mass includes a mass p , placed somewhere on the structure.

One can discover that when this mass, p , will be shifted now over a certain distance, c , as shown in figure 2.4-a, the original overall center of gravity G_0 will be shifted to G_1 - parallel to this displacement - over a distance equal to:

$$\overline{G_0G_1} = \frac{p \cdot c}{m} \tag{2.6}$$

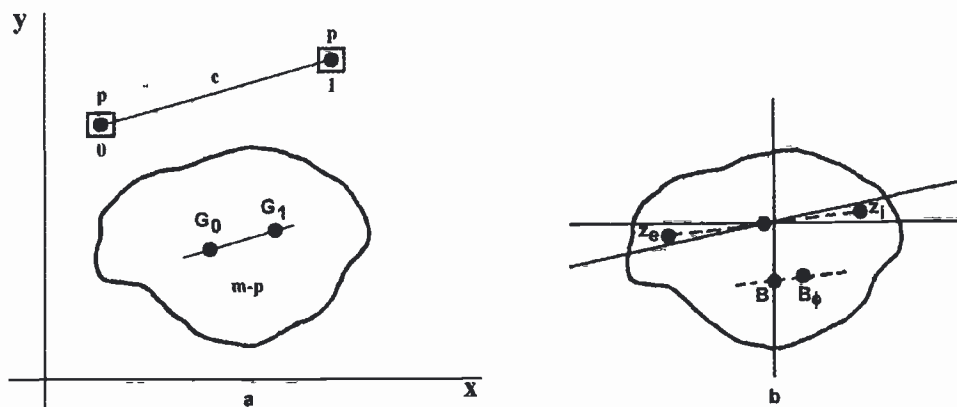


Figure 2.4: Shifting Mass and Buoyancy

One can also discover that the center of buoyancy shifts from B to B_ϕ parallel to a line $\overline{z_e z_i}$ through the centers of the volumes of the emerged and the immersed water displacement

'wedges' when a floating body heels by an external moment only. The volume of the emerged 'wedge', in fact, has been shifted to the immersed 'wedge'; see figure 2.4-b.

Because these two volumes are equal, two succeeding water planes with a small mutual difference in angle of heel intersect each other on a line with respect to which the first moments of volume of the two wedges are zero. This is a line through the center of the water plane. This means that the structure heels and/or trims about a line through the center of the water plane, the **center of floatation**. In case of a heeling ship (with symmetric water planes) this is a line at half the breadth of the water plane.

In case of a structure with vertical walls, the two 'wedges' become right angle triangles and the shift of the center of buoyancy from B to B_ϕ can be calculated easily.

Righting Moment of a Barge

Now we restrict our stability problems here to the case of a **rectangular barge** with length L , breadth B and draft T , heeling over a relatively **small heel angle**, ϕ . Then, the volume of displacement, ∇ , and the center of buoyancy, B , can be determined easily. The emerged and immersed wedges in the cross sections are bounded by vertical lines, so that these wedges are right angle triangles and the position of its centroids can be calculated easily.

Initially, the barge is floating in an upright even keel condition. Because of the rotational equilibrium in this condition, the center of gravity, G , is positioned on a vertical line through the center of buoyancy, B . If one adds now an (external) heeling moment M_H to this structure, it will heel with an angle ϕ ; see figure 2.5.

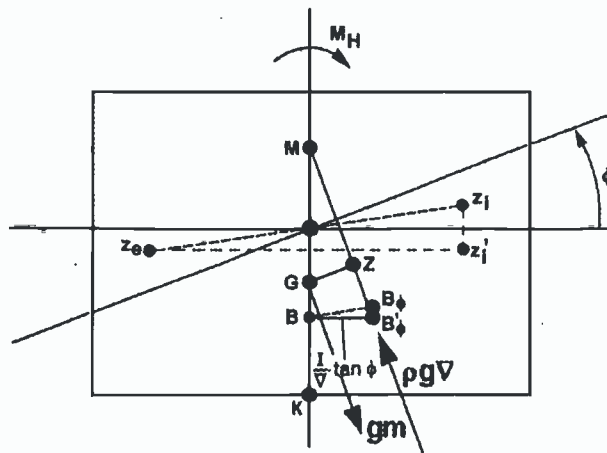


Figure 2.5: Rectangular Barge Stability

As a result of this heeling, the shape of the under water part of the structure will change; the center of buoyancy shifts from B to B_ϕ on a line parallel to the line through the centers of the emerged and immersed wedges $\overline{z_e z_i}$.

This shift of z_e of the emerged wedge to z_i of the immersed wedge can be split in two parts: a horizontal and a vertical shift. At small angles of heel ($\phi < 10^\circ$), the effect of the vertical shift on the stability can be ignored. Thus, it is assumed here that the vertical buoyancy force, $\rho g \nabla$, acts through point B'_ϕ in figure 2.5 (which is true for $\phi \rightarrow 0^\circ$).

The so-called **initial metacenter**, M , is defined as the point of intersection of the lines

through the vertical buoyant forces, $\rho g \nabla$, at a zero angle of heel and at a small angle of heel, ϕ .

An equilibrium will be achieved when the righting stability moment M_S equals the (external) heeling moment M_H :

$$M_S = \rho g \nabla \cdot \overline{GZ} = \rho g \nabla \cdot \overline{GM} \cdot \sin \phi = M_H \quad (2.7)$$

The position of the initial metacenter M can be calculated easily in our special case. This heeling causes a horizontal displacement of the center of buoyancy: $BB'_\phi = \overline{BM} \cdot \tan \phi$. The first moment of volumes with respect to the middle line plane of the barge in the heeled condition is given by:

$$\begin{aligned} \{LBT\} \cdot \{\overline{BM} \tan \phi\} &= \{LBT\} \cdot \{0\} + 2 \cdot \left\{ L \frac{1}{2} \frac{B}{2} \frac{B}{2} \tan \phi \right\} \cdot \left\{ \frac{2}{3} \frac{B}{2} \right\} \\ \text{new} &= \text{old} + \text{change} \end{aligned} \quad (2.8)$$

so that:

$$\overline{BM} = \frac{\frac{1}{12} \cdot L \cdot B^3}{L \cdot B \cdot T} = \frac{B^2}{12 \cdot T} \quad (\text{rectangular barge}) \quad (2.9)$$

or - more general - expressed in terms of the moment of inertia (second moment of areas) of the water plane, I_T , with respect to its center line and the displacement volume of the barge ∇ :

$$\overline{BM} = \frac{I_T}{\nabla} \quad (2.10)$$

The stability lever arm $\overline{GZ} = \overline{GM} \cdot \sin \phi$ will be determined by the hydrostatic properties of the submerged structure and the position of the center of gravity of this structure. This is reason why the following expression for \overline{GM} has been introduced:

$$\overline{GM} = \overline{KB} + \overline{BM} - \overline{KG} \quad (2.11)$$

where K is the keel point of the structure.

The magnitude of \overline{KB} follows from the under water geometry of the structure; for a rectangular barge:

$$\overline{KB} = \frac{T}{2} \quad (\text{rectangular barge}) \quad (2.12)$$

The magnitude of \overline{KG} follows from the mass distribution of the structure.

Numerical Application

A rectangular pontoon has the following principal dimensions: length $L = 60.00$ meter, breadth $B = 12.00$ meter and depth $D = 6.00$ meter.

The pontoon is floating at an even keel condition with a draft $T_0 = 2.50$ meter in sea water ($\rho = 1.025$ ton/m³). The vertical position of the centre of gravity of the pontoon, including fuel, above the base plane \overline{KG}_0 is 4.00 meter. A sketch of the pontoon in this situation is given in figure 2.6.

Then, a mass of $p = 65$ ton will be hoisted from the quay. When the derrick is turned outboard fully, the suspension point of the cargo in the derrick lies 13.00 meter above the base plane and 8.00 meter from the middle line plane of the pontoon.

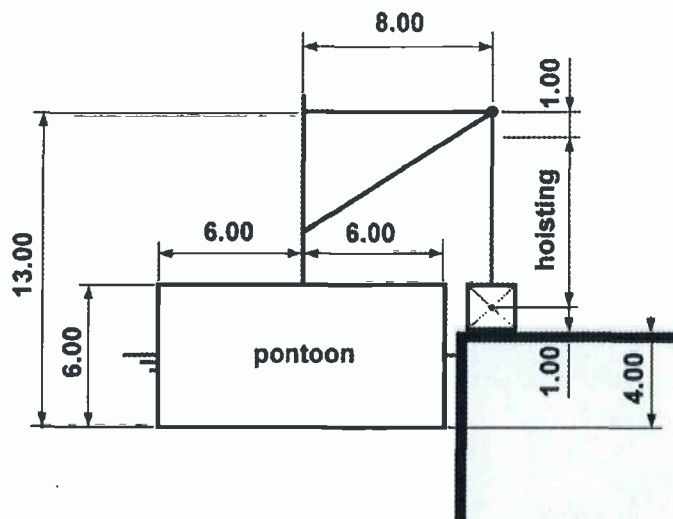


Figure 2.6: Lift Operation by a Pontoon

Question

Determine the maximum angle of heel of the pontoon during hoisting this load. The influence of the mass of the turning derrick may be ignored.

General Solution

Expecting a small angle of heel, the calculations will be carried out as follows:

1. Place the mass p above the centre of the water plane in a horizontal plane through the suspension point at the end of the derrick and, as a result of this, let the pontoon sink deeper parallel to the water plane. Determine in this situation the righting stability moment M_S in relation to the angle of heel ϕ :

$$M_S = \rho g \nabla \cdot \overline{GM} \cdot \sin \phi \quad (2.13)$$

2. Replace the shift of the mass p in a horizontal direction over a distance c to the actual place by a heeling moment M_H , which depends on the angle of heel ϕ too:

$$M_H = p \cdot g \cdot c \cdot \cos \phi \quad (2.14)$$

3. Finally, the equilibrium $M_S = M_H$ should be fulfilled:

$$\rho g \nabla \cdot \overline{GM} \cdot \sin \phi = p \cdot g \cdot c \cdot \cos \phi \quad (2.15)$$

From this all follows:

$$\tan \phi = \frac{p \cdot c}{\rho \nabla \cdot \overline{GM}} \quad (2.16)$$

Numerical Solution

Displacements of empty and laden pontoon:

$$\begin{aligned}\nabla_0 &= L \cdot B \cdot T_0 = 60.00 \cdot 12.00 \cdot 2.50 = 1800 \text{ m}^3 \\ \Delta_0 &= \rho \cdot \nabla_0 = 1.025 \cdot 1800 = 1845 \text{ ton} \\ \Delta &= \Delta_0 + p = 1845 + 65 = 1910 \text{ ton} \\ \nabla &= \frac{\Delta}{\rho} = \frac{1910}{1.025} = 1863 \text{ m}^3\end{aligned}$$

The under water hull form is a rectangular pontoon at an even keel condition without heel, so:

$$\begin{aligned}T &= \frac{\nabla}{L \cdot B} = \frac{1863}{60.00 \cdot 12.00} = 2.59 \text{ m} \\ \overline{KB} &= \frac{T}{2} = \frac{2.59}{2} = 1.29 \text{ m} \\ \overline{BM} &= \frac{I_T}{\nabla} = \frac{B^2}{12 \cdot T} = \frac{12.00^2}{12 \cdot 2.59} = 4.63 \text{ m}\end{aligned}$$

The vertical position of the centre of gravity of the laden pontoon follows from the first moment of masses with respect to the base plane:

$$\Delta \cdot \overline{KG} = \Delta_0 \cdot \overline{KG_0} + p \cdot z_p$$

So:

$$\begin{aligned}\overline{KG} &= \frac{\Delta_0 \cdot \overline{KG_0} + p \cdot z_p}{\Delta} \\ &= \frac{1845 \cdot 4.00 + 65 \cdot 13.00}{1910} = 4.31 \text{ m}\end{aligned}$$

Herewith, the initial metacentric height is known:

$$\begin{aligned}\overline{GM} &= \overline{KB} + \overline{BM} - \overline{KG} \\ &= 1.29 + 4.63 - 4.31 = 1.61 \text{ m}\end{aligned}$$

As pointed out before, an equilibrium will be achieved when the righting stability moment M_S equals the heeling moment M_H :

$$\tan \phi = \frac{p \cdot c}{\rho \nabla \cdot \overline{GM}} = \frac{65 \cdot 8.00}{1910 \cdot 1.61} = 0.169 \quad \text{thus: } \phi = 9.6^\circ$$

Static Stability Curve

The stability lever arm definition, $\overline{GZ} = \overline{GM} \cdot \sin \phi$, used here is valid for structures with vertical side walls of the hull in the 'zone between water and wind', having small angles of heel only.

For practical applications it is very convenient to present the stability in the form of righting moments or lever arms about the center of gravity G , while the floating structure is heeled at a certain displacement, ϕ . This is then expressed as a function of ϕ . Such a function

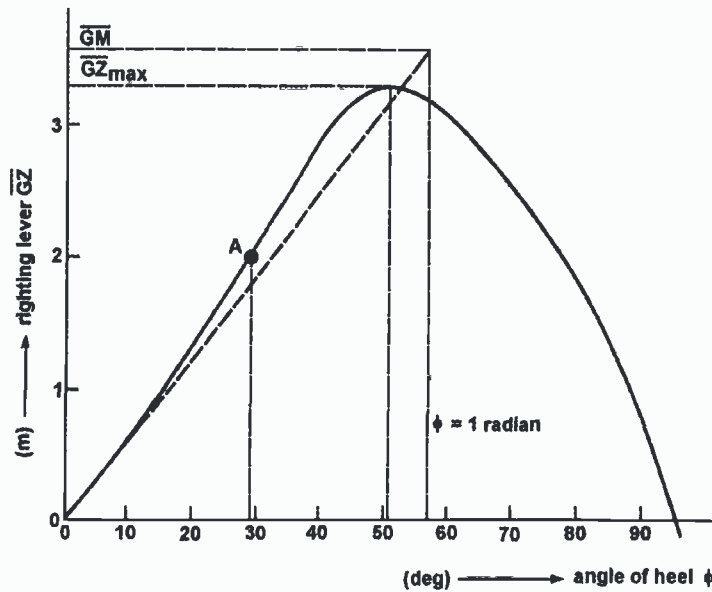


Figure 2.7: Ship Static Stability Curve

will generally look something like figure 2.7 and is known as the **static stability curve** or the **GZ-curve**.

Because the stability lever arm is strongly dependent on the angle of heel, ϕ , a graph of \overline{GZ} , as given in figure 2.7 is very suitable for judging the static stability at any angle of heel. It is obvious that for symmetric forms like ships, the curve of static stability **will** be symmetric with respect to $\phi = 0$. In that case, only the right half of this curve will be presented as in figure 2.7.

At small angles of heel this \overline{GZ} -curve follows $\overline{GZ} = \overline{GM} \cdot \sin \phi \approx \overline{GM} \cdot \phi$, as discussed here. At increasing heel angles, the effect of the vertical shift of the center of buoyancy, B_ϕ , starts to play a role; it increases the stability lever arm a bit. At larger angles of heel the shape of structure becomes important; no vertical side walls, deck enters in the water, bilge comes out of the water, etc. This decreases the stability lever arm drastically. The heel angle at point A in this figure, at which the second derivative of the curve changes sign, is roughly the angle at which the increase of stability due to side wall effects starts to be counteracted by the fact that the deck enters the water or the bilge comes above the water.

Free Surface Correction

Free surfaces of liquids inside a floating structure can have a large influence on its static stability; they reduce the righting moment or stability lever arm. When the structure heels as a result of an external moment M_H , the surface of the fluid in the tank remains horizontal. This means that this free surface heels relative to the structure itself, so that the center of gravity of the structure (including liquid) shifts.

This effect can not be ignored when judging a structure's safety.

Chapter 3

Resistance and Propulsion

3.1 Scaling

Physical model experiments require some form of similarity between the prototype and the model:

- **Geometric similarity:** The model must have physical dimensions which are uniformly proportional to those of the prototype; it must have the same shape.
- **Kinematic similarity:** Velocities in the model must be proportional to those in the prototype.
- **Dynamic similarity:** Forces and accelerations in the model must be proportional to those in the prototype.

These three similarities require that all location vectors, velocity vectors and force vectors in the coincident coordinates of the scaled model and the prototype have the same direction (argument) and that the magnitude of these vectors (modulus) must relate to each other in a constant proportion.

Reynolds Scaling

Reynolds scaling is used when inertia and viscous forces are of predominant importance in the flow. This is the case for pipe flow (under pressure) and for wake formation behind a body in a flow. Reynolds scaling requires that the Reynolds number in the model be identical to that in the prototype. This Reynolds number represents the ratio of:

$$Rn = \frac{\text{inertia forces}}{\text{viscous forces}} = \frac{V \cdot L}{\nu} \quad \text{Reynolds number} \quad (3.1)$$

Froude Scaling

Gravity forces become important when a free surface of a fluid is involved. This will be true, then when the ocean surface or waves are present - very commonly in offshore engineering practice, therefore. This makes it appropriate to keep the ratio of inertia or pressure force and inertia forces the same in the model as in the prototype. Scaling based upon the square root of this ratio is called Froude scaling, after Robert Edmund Froude (as distinct from his father William Froude from the model resistance extrapolation to full scale, treated in a following section) who has first used it. This Froude number represents the ratio of:

$$Fn = \sqrt{\frac{\text{inertia or pressure forces}}{\text{gravity forces}}} = \frac{V}{\sqrt{gL}} \quad \text{Froude number} \quad (3.2)$$

Scale Effect

As an example, suppose a ship with a length $L_s = 100$ meter, which sails with a forward ship speed V of 20 knots in still seawater with a temperature of 15°C . Resistance and propulsion tests will be carried out in a towing tank with a 1:40 scale physical model ($\alpha = 40$).

The temperature of the fresh water in the tank is 20°C . The density and the kinematic viscosity of sea water are $\rho = 1025.9 \text{ kg/m}^3$ and $\nu = 1.19 \cdot 10^{-6} \text{ m}^2/\text{s}$. The relevant values for fresh water are $\rho = 998.1 \text{ kg/m}^3$ and $\nu = 1.05 \cdot 10^{-6} \text{ m}^2/\text{s}$.

The length of the ship model is:

$$L_m = \frac{L_s}{\alpha} = \frac{100}{40} = 2.50 \text{ m} \quad (3.3)$$

According to Newton's law, the inertia forces are defined as a product of mass and acceleration. From this follows that one can write for these forces:

$$F_s = C \cdot \frac{1}{2} \rho_s V_s^2 \cdot L_s^2 \quad \text{and} \quad F_m = C \cdot \frac{1}{2} \rho_m V_m^2 \cdot L_m^2 \quad (3.4)$$

in which the coefficient, C , does not depend on the scale of the model nor on the stagnation. The speed V_s of the ship is:

$$V_s = 0.5144 \cdot V = 0.5144 \cdot 20 = 10.29 \text{ m/s} \quad (3.5)$$

Because gravity waves play the most important role during these tests, but also for practical reasons, the speed of the model will be obtained using Froude scaling:

$$Fn_s = \frac{V_s}{\sqrt{g \cdot L_s}} = \frac{10.29}{\sqrt{9.81 \cdot 100}} = 0.329 = Fn_m \quad (3.6)$$

So:

$$V_m = Fn_m \cdot \sqrt{g \cdot L_m} = 0.329 \cdot \sqrt{9.81 \cdot 2.50} = 1.63 \text{ m/s} \quad (3.7)$$

A consequence of this scaling is that the Reynolds numbers will differ:

$$\begin{aligned} Rn_s &= \frac{V_s \cdot L_s}{\nu_{\text{salt}}} = \frac{10.29 \cdot 100}{1.19 \cdot 10^{-6}} = 865 \cdot 10^6 \\ Rn_m &= \frac{V_m \cdot L_m}{\nu_{\text{fresh}}} = \frac{1.63 \cdot 2.50}{1.05 \cdot 10^{-6}} = 3.88 \cdot 10^6 \end{aligned} \quad (3.8)$$

To obtain equal Reynolds numbers, the "model water" needs a kinematic viscosity which is 1/223 times its actual value; this liquid is not available!

When experimentally determining the resistance and propulsion characteristics of ships on the surface of a fluid, Froude scaling is still used from a practical point of view. This means, however, that the viscous forces on the model will still be much more important than those on the ship. This so called **scale effect** means that the constant C in the general expression for the force, (equation 3.4) is not the same for model and prototype. Extrapolation of model resistance test data to full scale data and the performance of propulsion tests require special attention, as will be discussed in this chapter.

3.2 Resistance

It has been the merit of William Froude, 1810 - 1878, (as distinct from his son Robert Edmund Froude from the Froude number) to distinguish the components of the **total hull resistance**, R_t , and to relate them to scaling laws. He distinguished between a **frictional resistance** component, R_f , and a **residual resistance** component, R_r . Then he made a very drastic simplification, which has worked out remarkably well. Froude's first hypothesis was that these two components of the resistance are independent of each other. The determination of these two components was a second problem, but he found a simple way out of this problem. Froude's second hypothesis was that the frictional part of the resistance can be estimated by the drag of a flat plate with the same wetted area and length as the ship or model. In principle, a flat plate (towed edgewise) has no wave resistance and can therefore be investigated over a range of Reynolds numbers ($Rn = VL/\nu$) without influence of the wave-related Froude number ($Fn = V/\sqrt{gL}$).

Resistance Components

The determination of the resistance components of a ship's hull can be illustrated with the results of resistance tests with a series of models at various scales, the "Simon Bolivar" family of models. Resistance tests were carried out over a certain speed range for each of the models. Each model had a different scale factor, α . The total resistance (in non-dimensional form) is shown in figure 3.1.

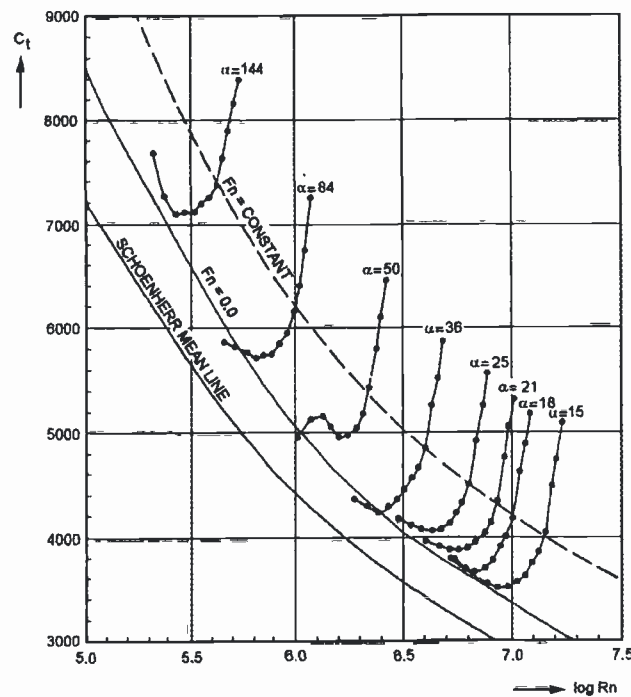


Figure 3.1: Resistance Coefficients of the "Simon Bolivar" Model Family

The total resistance force on a ship is made non-dimensional by:

$$C_t = \frac{R_t}{\frac{1}{2}\rho V^2 S} \quad \text{or:} \quad R_t = \frac{1}{2}\rho V^2 \cdot C_t \cdot S \quad (3.9)$$

in which C_t is the total resistance coefficient (-), R_t is the total resistance (N), ρ is the density of water (kg/m^3), V is the ship or model speed (m/s) and S is the wetted surface of ship or model hull (m^2).

C_t is plotted as a function of the logarithm of the Reynolds number, $Rn = VL/\nu$. Each curve of data points has been made with a model of the given scale. The frictional part of the resistance is given by the Schoenherr plate line, treated in the next section; the other two curves connects the points for F_n is zero and for F_n is another constant, respectively. Similar lines can be drawn at other Froude numbers. Such a line of constant Froude number is approximately parallel to the Schoenherr plate line. If all scaling laws could be satisfied, the resistance curves at all model scales would coincide. Because the Reynolds number is not maintained, this is not the case and each model has a separate curve.

Frictional Resistance Component To determine the frictional resistance coefficient, William Froude's approach yielded that the frictional resistance coefficient was related to the resistance coefficient of a flat plate with the same length and wetted surface as the ship or model hull:

$$C_f = \frac{R_f}{\frac{1}{2}\rho V^2 S} \quad \text{or} \quad R_f = \frac{1}{2}\rho V^2 \cdot C_f \cdot S \quad (3.10)$$

in which C_f is the frictional resistance coefficient (-), R_f is the frictional resistance (N), ρ is the density of water (kg/m^3), V is the ship or model speed (m/s) and S is the wetted surface of ship or model hull (m^2).

He did numerous experiments to determine the resistance coefficients of a flat plate as a function of the Reynolds number. He himself did not find a single relationship as a function of the Reynolds number due to laminar flow and edge effects in his measurements. His results not only depended on the Reynolds number but also on the length of the plate. Several friction lines based only on the Reynolds number were developed later, both theoretically using boundary layer theory and experimentally.

So-called plate lines were developed for turbulent boundary layer flows from the leading edge. These lines were extended to include full scale Reynolds numbers. They have relatively simple formulations, such as the **Schoenherr Mean Line** or the **ITTC-1957 Line**, which are defined as:

$$\text{Schoenherr:} \quad \frac{0.242}{\sqrt{C_f}} = \log_{10}(Rn \cdot C_f) \quad (3.11)$$

$$\text{ITTC-1957:} \quad C_f = \frac{0.075}{(\log_{10}(Rn) - 2)^2} \quad (3.12)$$

The latter one is accepted as a standard by the International Towing Tank Conference (ITTC). As a matter of fact it is not too important that a flat plate with a certain length and wetted surface has a resistance coefficient exactly according to one of the mentioned lines. The Froude hypothesis is already very crude and correlation factors are required afterwards to arrive at correct extrapolations to full scale values. These correlation factors will depend on the plate line which is used.

Residual Resistance Component The residual resistance coefficient, C_r , at a certain Froude number is now the vertical distance between the plate line and the line for that Froude number. When the plate line and the line of constant Froude number are parallel,

this means that the residual resistance component is indeed independent of the Reynolds number. This is assumed to be always the case in Froude's method and the residual resistance at each Froude number is determined by subtracting the calculated frictional resistance coefficient of a flat plate according to equations 3.11 or 3.12 from the measured total resistance.

Extrapolation of Resistance Tests

Given the components of the total resistance of the model, one must extrapolate this data to full scale. The resistance of the model is generally measured from a low speed up to the design speed. The model design speed is set by maintaining the full scale Froude number. Equation 3.9 is used to express the total resistance in dimensionless form. Froude scaling is maintained during the model test. This means that the residual resistance coefficient, C_r , at model scale and at full scale are the same.

The total resistance coefficient of the ship, $C_{t \text{ ship}}$, can therefore be found from:

$$C_{t \text{ ship}} = C_{f \text{ plate line}} + C_{r \text{ model}} \quad (3.13)$$

and the total resistance of the ship follows from:

$$R_{t \text{ ship}} = \frac{1}{2} \rho V^2 \cdot C_{t \text{ ship}} \cdot S \quad (3.14)$$

Resistance Prediction Methods

A number of methods to determine the still water resistance coefficients of ships, based on (systematic series of) model test data, are given in the literature. A very well known method, developed at MARIN, is described by [Holtrop, 1977], [Holtrop and Mennen, 1982] and [Holtrop, 1984]. The method is based on the results of resistance tests carried out by MARIN during a large number of years and is available in a computerized format. The reader is referred to these reports for a detailed description of this method, often indicated by the "Holtrop and Mennen" method.

An example for a tug of the correlation between a resistance prediction method and a prediction with model test results is given in figure 3.2.

3.3 Propulsion

The basic action of propulsors like propellers is to deliver thrust. In fact, a propulsor is an **energy transformer**, because **torque and rotation**, delivered to the propulsor, will be transformed into **thrust and translation**, delivered by the propulsor. A consequence is that the propulsor also generates water velocities in its wake, which represent a loss of kinetic energy. It is obvious that this will effect the **efficiency** of the propulsor, defined by:

$$\eta = \frac{P_{out}}{P_{in}} = \frac{P_E}{P_D} = \frac{T \cdot V_e}{Q \cdot 2\pi n} \quad (3.15)$$

in which η is the propulsive efficiency (-), P_D is the **delivered power**, delivered to the propulsor (Nm/s = W), P_E is the **effective power**, delivered by the propulsor (Nm/s = W), Q is the torque delivered to the propulsor (Nm), n is the number of revolutions (1/s),

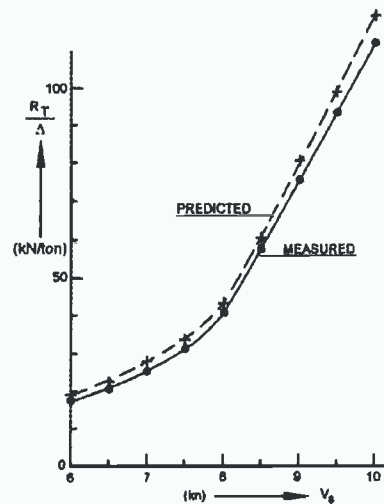


Figure 3.2: Comparison of Resistance Prediction with Model Test Results

T is the thrust delivered by the propulsor (N) and V_e is the mean entrance speed of water in propeller disk, also called advance velocity with notation V_a (m/s).

The efficiency varies widely between various types of propulsors, but the screw propeller has not yet been equalled in most cases and is therefore the most commonly used propulsor. The propulsor is generally mounted behind the hull. This is because of efficiency; the water which is brought into motion by the friction along the ship is reversed by the propeller action and as a result less energy is left behind in the water.

A risk for every propulsor operating at high rotational velocities is cavitation. This occurs when the local pressure, associated with high local velocities in the fluid, is lower than the vapor pressure. When these vapor-filled (not air-filled) cavities in the wake arrive in regions with a higher pressure they collapse violently, causing local shock waves in the water that can erode the nearby surface. This dynamic behavior of large cavities can also generate vibrations in the ship structure.

Propulsors

The most important propulsors used for shipping and offshore activities include:

- **Fixed Pitch Propellers**, see figure 3.3-a.

The most common propulsor is the fixed pitch open screw propeller (FPP) which, as all propellers, generates a propulsive force by lift on the propeller blades. These blade sections are similar to those of airfoils, operating at some angle of attack in the flow. The geometry of the propeller blades is quite critical due to the occurrence of cavitation. Therefore, a specific propeller is generally designed for the specific circumstances of each ship and its engine. The thrust, and consequently the speed of the ship, is controlled by the propeller rotational speed - often called revolutions or rpm (for revolutions per minute).

- **Controllable Pitch Propellers**, see figure 3.3-b.

In case of a controllable pitch propeller (CPP) the thrust is controlled by changing the pitch of the blades. In this case the shaft often has a constant rotational speed. Such a propeller is often used when the propeller has to operate at more than one condition

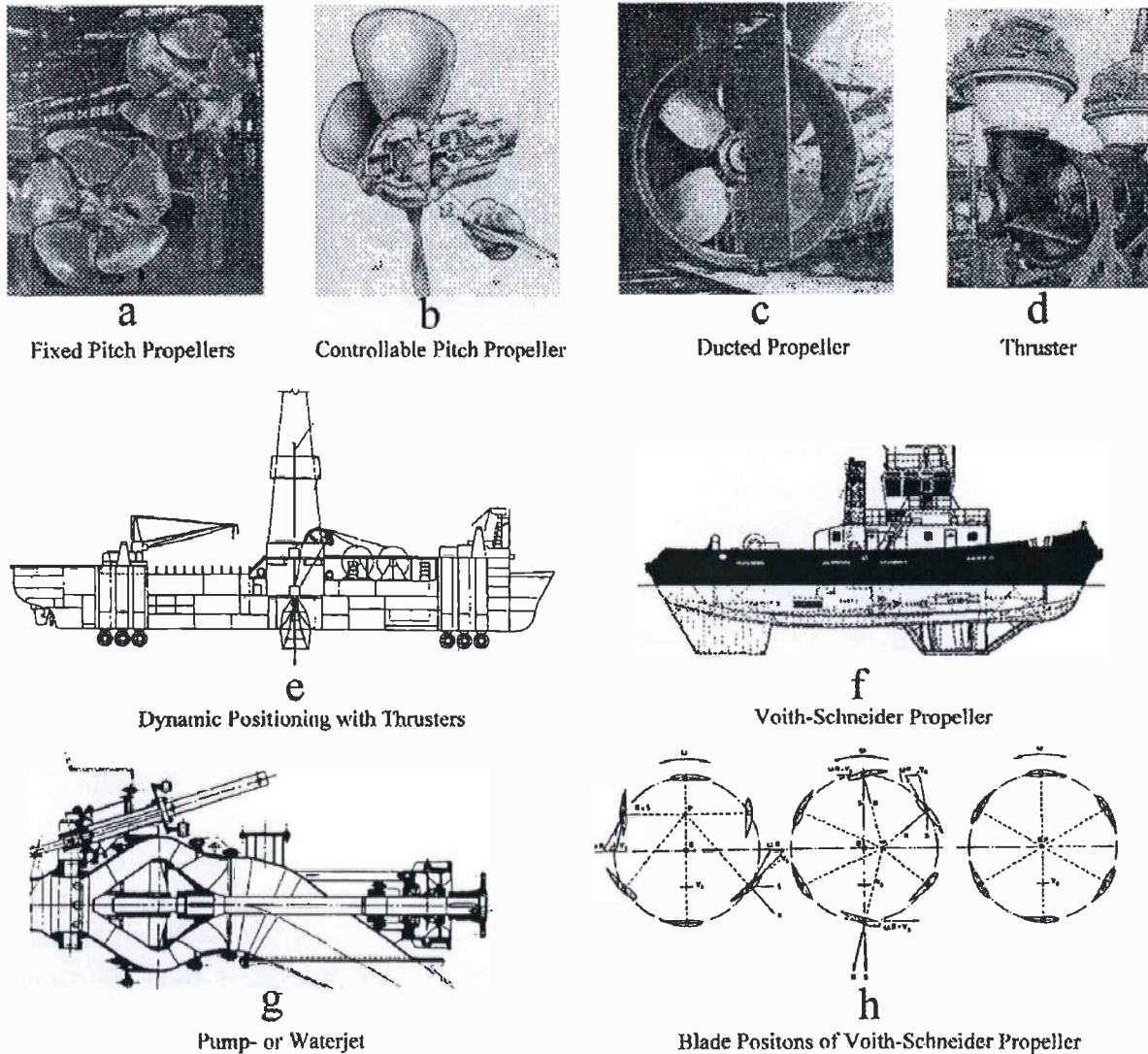


Figure 3.3: Different Propulsion Configurations

- such as free running and towing. It is also effective when rapid manoeuvring is required or when shaft generators, which require a constant rpm, are present. Reversing the thrust occurs by changing the pitch with constant revolutions in the same direction. This significantly decreases the time required to change the direction of the thrust. It is important to keep in mind that the CPP has only one design pitch; changing the pitch always reduces the efficiency.

- **Ducted Propellers**, see figure 3.3-c.

At high propeller loadings a duct increases the propeller efficiency. A duct generates part of the total thrust due to its interaction with the propeller. This is the case with an accelerating duct, in which the flow velocity is increased due to the duct. Ducted propellers are used in a wide range of applications with heavily loaded propellers, such as for tugs. Several types of ducts, sometimes asymmetric and sometimes at some distance upstream of the propeller, have been designed to make the propeller inflow more uniform.

- **Thrusters**, see figures 3.3-d and 3.3-e.

A propeller can be driven from above by a vertical shaft. This makes it possible to rotate the propeller along the vertical axis and to generate thrust in any chosen direction. These configurations are called thrusters. They can have an open propeller, but very often a duct is also used. The right angle drive of a thruster makes it more complicated and thus more expensive and vulnerable than a normal propeller shaft. Also the hub diameter is larger, which slightly decreases efficiency. On the other hand, a thruster has advantages too. The propeller can be in front of the vertical shaft (towing) as well as behind it (pushing). In the towing mode the inflow is more uniform; this decreases vibrations and cavitation. A steerable or azimuthing thruster may rotate around a vertical axis which makes it possible to steer with it. This makes it easier to manoeuvre, especially at low speeds. They are common for dynamic positioning; the steerable direction of its thrust is fully utilized in that case.

- **Cycloidal or Voith-Schneider Propellers**, see figures 3.3-f and 3.3-h.

A very special propulsor is the cycloidal propeller, also called Voith-Schneider propeller after its main developer. It consists of a number of foils on a rotating plate. These foils can rotate relative to this plate and their position is such that they are always perpendicular to the radii from a moving center point, P , as shown in figure 3.3-h. When this center point is in the center of the blade circle, there is no resulting force. When this center point is moved, a thrust is generated perpendicular to the direction in which the center point is shifted. Thus thrust can be applied in any direction just by moving the center point; rudders can be omitted. This propulsive system can be used for tugs and supply boats, for which maneuvering is important. Its efficiency, however, is lower than that of an open propeller due to the fact that the blades generate thrust over a part of their revolution only, while viscous resistance is present over the whole revolution. Voith-Schneider propellers must be mounted under a flat bottom; a bottom cover is sometimes provided for protection (see figure 3.3-f).

- **Water Jets**, see figure 3.3-g.

This propulsor accelerates water using a pump inside the hull, instead of a propeller outside the hull. The water is drawn in from the bottom of the ship, is accelerated inside the ship by a pump and leaves the ship at the stern. This has many advantages when a propeller is too vulnerable to damage, or when a propeller is too dangerous as is the case for rescue vessels. Rudders can be omitted because of the rotating possibilities of the outlet and excellent manoeuvring qualities can be obtained, as for instance are required for pilot vessels. A pump jet can be useful in shallow water. However, the inner surface of the pump system is large and the velocities inside are high; the viscous losses are high, too. The efficiency is therefore lower than that of an open propeller.

Propeller Geometry

Consider now an arbitrary propeller as drawn in figure 3.4-a. The intersection of a cylinder with radius r and a propeller blade, the blade section has the shape of an airfoil. Such a shape is also called just a foil or a profile. The blade sections of the propeller have a certain pitch. The chord line or nose-tail line of the blade section - a helix on the cylinder - becomes a straight pitch line, if the cylinder is developed on to a flat surface. The propeller

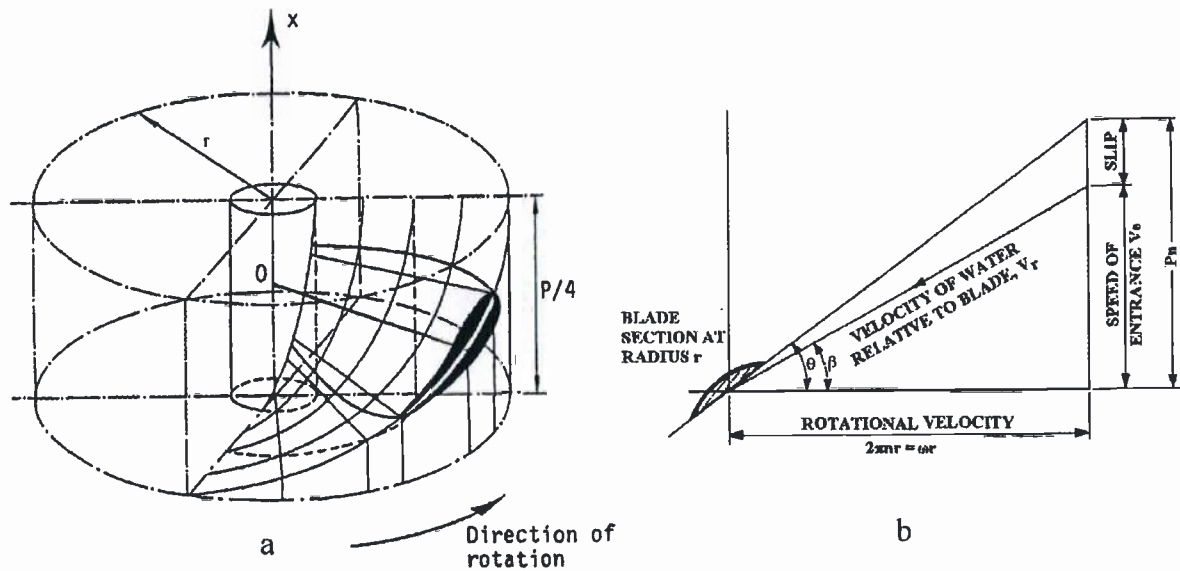


Figure 3.4: Propeller Geometry

pitch, P , is defined as the increase in axial direction of the pitch line over one full revolution $2\pi r$ at each radius r . The dimension of the pitch is a length. The ratio P/D is the pitch ratio. The pitch angle, $\theta = \arctan(P/2\pi r)$, is the angle between the pitch line and a plane perpendicular to the propeller shaft.

Figure 3.4-b shows the axial velocity V_e and rotational velocity $2\pi nr$ of the water particles at a radius r from the propeller axis. As a propeller is rotating in water, it can not advance $P \cdot n$ and a certain difference occurs. The difference between $P \cdot n$ and V_e is called the slip of the propeller.

A significant radius, which is often used as representative for the propeller, is the radius at $r/R = 0.7$. If a pitch is given in the case of a variable pitch distribution it is usually the pitch at $0.7R$. Note that half the area of the propeller disk is within a circle with radius $0.7R$ and that, consequently, the other half is outside this region; so the pressure at this circular line is "more or less" the average pressure over the full propeller disk.

Another important parameter of the propeller is the expanded blade area ratio, given as the ratio between the expanded area, A_E , of all blades and the area of the propeller plane, $A_0 = 0.25\pi D^2$.

Open Water Characteristics

Suppose an open water propeller translating with a constant forward speed, V_e , and a constant number of revolutions per second, n , is immersed in a homogeneous initially stationary fluid without any currents or waves. Then, two velocity components can be defined for this propeller: a rotational velocity, $2\pi nr$, at a certain radius, r , and an axial translation velocity, V_e . The hydrodynamic pitch angle, β , of the flow relative to the blade sections is generally taken at $r = 0.7R$, just as was done to define the pitch:

$$\beta_{0.7R} = \arctan \left(\frac{V_e}{0.7\pi \cdot nD} \right) \tag{3.16}$$

An important parameter to describe the angle of attack, and therefore the lift and drag, is the advance ratio, J , defined by:

$$J = \frac{V_e}{nD} \quad (3.17)$$

The resistance of a ship was made non-dimensional in equation 3.9 by:

$$C_t = \frac{R}{\frac{1}{2}\rho V^2 S} = \frac{R}{\frac{1}{2}\rho \cdot (\text{velocity})^2 \cdot (\text{area})} \quad (3.18)$$

When using the rotational velocity at for instance $0.7R$ as a characteristic velocity and the area of the propeller disk as a characteristic area, the thrust of a propeller can be made non-dimensional in the same way by:

$$C_T = \frac{T}{\frac{1}{2}\rho \cdot (0.7\pi \cdot nD)^2 \cdot \left(\frac{\pi}{4}D^2\right)} \approx \frac{16.33}{\pi^3} \cdot \frac{T}{\rho D^4 n^2} \quad (3.19)$$

The constant $16.33/\pi^3$ can be included in the constant C_T and so the **thrust coefficient** becomes:

$$K_T = \frac{T}{\rho D^4 n^2} \quad \text{or:} \quad T = K_T \cdot \rho D^4 n^2 \quad (3.20)$$

and the **torque coefficient** can be written in a similar way as:

$$K_Q = \frac{Q}{\rho D^5 n^2} \quad \text{or:} \quad Q = K_Q \cdot \rho D^5 n^2 \quad (3.21)$$

in which K_T is the thrust coefficient (-), K_Q is the torque coefficient (-), T is the thrust (N), Q is the torque (Nm), ρ is the density of water (kg/m^3), D is the diameter (m) and n is the revolution speed (1/s).

These propeller performance characteristics, K_T and K_Q , in a uniform flow are given in figure 3.5.

The power delivered to the propeller is the **delivered power** P_D :

$$P_D = Q \cdot 2\pi n \quad (3.22)$$

The power delivered by the thrust is the **effective power** P_E :

$$P_E = T \cdot V_e \quad (3.23)$$

The **efficiency** of the open water propeller is the ratio between effective and delivered power:

$$\eta_O = \frac{P_E}{P_D} = \frac{T \cdot V_e}{Q \cdot 2\pi n} \quad \text{or:} \quad \eta_O = \frac{K_T}{K_Q} \cdot \frac{J}{2\pi} \quad (3.24)$$

In addition to the thrust and torque coefficients, K_T and K_Q , the propulsive efficiency of the open water propeller, η_O , is shown in figure 3.5 too.

Ship Propulsion

This section treats the behavior of the **propeller behind the ship** and its interaction with the ship.

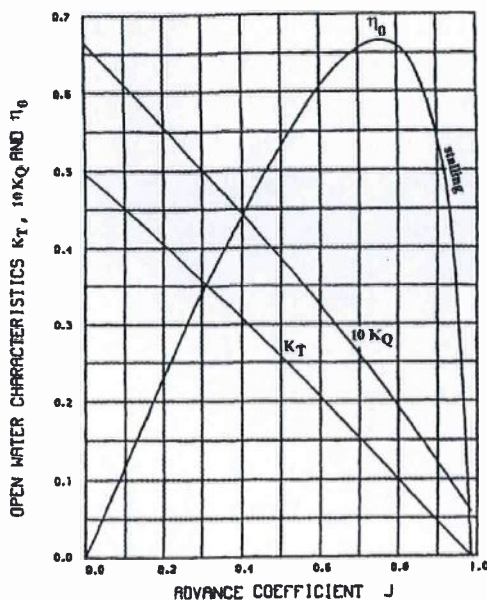


Figure 3.5: Open Water Propeller Diagram

Wake Fraction The velocity deficit behind the ship is a measure of its still water resistance. The velocity deficit in the propeller plane (without the propeller present) can be integrated and averaged over the propeller plane. This velocity is the average entrance velocity, V_e , in the propeller plane when the propeller is absent. It is defined in terms of the ship speed, V_s , by the nominal wake fraction, w_n :

$$w_n = \frac{V_s - V_e}{V_s} \tag{3.25}$$

This definition is a non-dimensional form of the velocity deficit, $V_s - V_e$, in the propeller plane. Unsteady effects will be neglected now and the (average) nominal wake fraction will be used to obtain the (constant) open water propeller inflow, which yields the entrance velocity:

$$V_e = V_s \cdot (1 - w) \quad \text{with: } w = w_n \tag{3.26}$$

Thrust Deduction Fraction The propeller has an effect on the ship's resistance, however. It increases the resistance of the ship by increasing the velocity along the hull (generally a small effect) and by decreasing the pressure around the stern. The increase of resistance due to the propeller action is expressed as the thrust deduction fraction, t :

$$t = \frac{T - R}{T} \tag{3.27}$$

where T is the thrust needed to maintain a certain design speed and R is the resistance without propeller at that speed, as found from resistance tests.

With this, the relation between resistance and thrust is:

$$R = T \cdot (1 - t) \tag{3.28}$$

Propulsive Efficiency The total efficiency is the ratio of the useful energy delivered by a system (output) and the energy supplied to the system (input). For the ship with propeller the output is $R \cdot V_s$ and the input is $Q \cdot \omega = Q \cdot 2\pi n$.

This total propulsive efficiency can be divided into parts which are related to the propeller performance without the hull and to the hull without the propeller:

$$\begin{aligned}
 \eta_T &= \frac{R \cdot V_s}{Q \cdot 2\pi n} \\
 &= \frac{T(1-t) \cdot \frac{V_e}{1-w}}{\frac{Q}{Q_0} \cdot Q_0 \cdot 2\pi n} \\
 &= \left(\frac{T \cdot V_e}{Q_0 \cdot 2\pi n} \right) \cdot \left(\frac{1-t}{1-w} \right) \cdot \left(\frac{Q_0}{Q} \right) \\
 &= \left(\frac{K_T}{K_Q} \cdot \frac{J}{2\pi} \right) \cdot \left(\frac{1-t}{1-w} \right) \cdot \left(\frac{Q_0}{Q} \right) \quad (3.29)
 \end{aligned}$$

or:

$$\eta_T = \eta_O \cdot \eta_H \cdot \eta_R$$

in which, at the same thrust, Q_0 is the torque of the open water propeller in a uniform flow and Q is the torque of the propeller in the wake behind the ship.

The total propulsive efficiency is thus divided into three components:

- **Open Water Efficiency:**

$$\eta_O = \frac{T \cdot V_e}{Q_0 \cdot 2\pi n} = \frac{K_T}{K_Q} \cdot \frac{J}{2\pi} \quad (3.30)$$

This is the efficiency of the propeller alone in the mean (homogeneous) inflow, V_e . It can be derived from open water diagrams of propellers.

- **Hull Efficiency:**

$$\eta_H = \frac{R \cdot V_s}{T \cdot V_e} = \frac{1-t}{1-w} \quad (3.31)$$

Old but convenient rough approximations of the wake fraction and the thrust deduction fraction of full scale ships are given by:

$$w \approx 0.5 \cdot C_B - 0.05 \quad \text{and} \quad t \approx 0.6 \cdot w \quad (3.32)$$

where C_B is the block coefficient of the ship.

A fast slender container vessel with $C_B = 0.55$ will have $\eta_H \approx 1.12$ while for a crude oil carrier with $C_B = 0.85$, $\eta_H \approx 1.24$. So the effect of a hull with its wake before the propeller increases the propulsive efficiency considerably. The propeller diameter therefore has to be such that the wake is going through the propeller disk as much as possible.

When using model data, it should be noted that - contrarily to the thrust deduction fraction - the wake fraction is very sensitive for scale effect.

- **Relative Rotative Efficiency:**

$$\eta_R = \frac{Q_o}{Q} \quad (3.33)$$

This efficiency reflects the difference in torque in the wake and in open water at the same thrust. The relative rotative efficiency is generally close to one; $\eta_R = 0.98 - 1.00$ for single-screw ships and $\eta_R = 1.00 - 1.02$ for twin-screw ships.

3.4 Propulsion versus Resistance

A very practical offshore engineering application of the information from the latter sections of this chapter involves the prediction of the speed at which a barge (or other floating object) will be towed by a given tugboat. Such information can be invaluable for the logistic planning of a major offshore operation.

A tugboat will of course be able to deliver more thrust than it needs to overcome its own frictional and wave making resistance. In general, the available towing force which a tugboat can deliver will be a function of its towing speed. This function, which decreases with increasing speed, will be known for the tug selected. In general, each tug will have a family of curves depending upon the speed of its engine. On the other hand, only one engine speed will deliver the highest overall efficiency for any given speed.

The resistance for the towed object should be known as well. This resistance force will generally be an increasing function of towing velocity. Superposition of the two curves - one for the tugboat and one for the towed object will yield the optimum towing speed. This is the speed corresponding to the intersection point of the two curves; see figure 3.6.

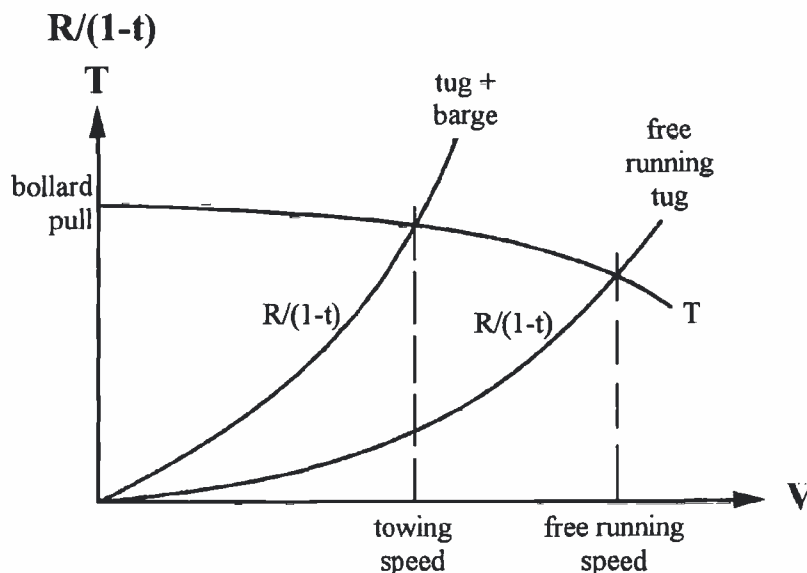


Figure 3.6: Free Running and Towing Speed of a Tug

Chapter 4

Summary of Ocean Surface Waves

Ocean surface waves cause periodic loads on all sorts of man-made structures in the sea. It does not matter whether these structures are fixed or floating and on the surface or deeper in the sea. A summary of the most relevant phenomena is given here.

4.1 Regular Waves

Figure 4.1 shows a harmonic wave as seen from two different perspectives. Figure 4.1-a shows what one would observe in a snapshot photo made looking at the side of a (transparent) wave flume; the wave profile is shown as a function of distance x along the flume at a fixed instant in time. Figure 4.1-b is a time record of the water level observed at one location along the flume; it looks similar in many ways to the other figure, but time t has replaced x on the horizontal axis.

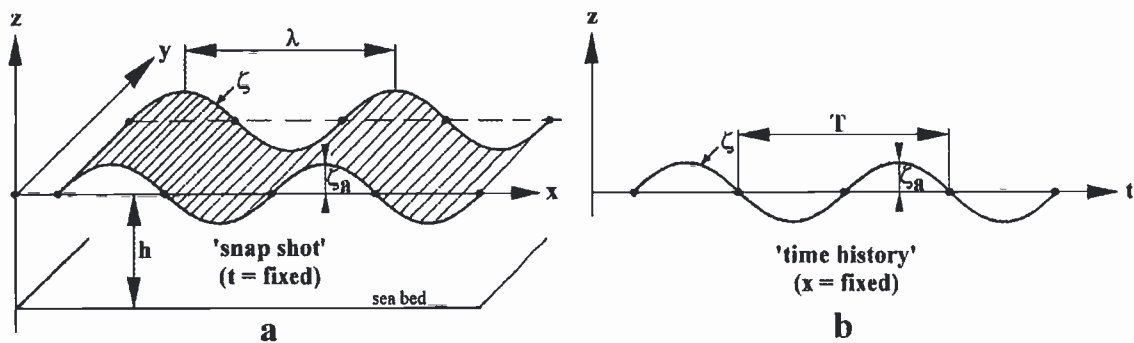


Figure 4.1: Harmonic Wave Definitions

Notice that the origin of the coordinate system is at the still water level with the positive z -axis directed upward; most relevant values of z will be negative. The still water level is the average water level or the level of the water if no waves were present. The x -axis is positive in the direction of wave propagation. The water depth, h , (a positive value) is measured between the sea bed ($z = -h$) and the still water level.

The highest point of the wave is called its crest and the lowest point on its surface is the trough. If the wave is described by a sine wave, then its amplitude ζ_a is the distance from the still water level to the crest, or to the trough for that matter. The subscript a denotes

amplitude, here. The wave height H is measured vertically from wave trough level to the wave crest level, it is the double amplitude.

The horizontal distance (measured in the direction of wave propagation) between any two successive wave crests is the wave length, λ . The distance along the time axis is the wave period, T . The ratio of wave height to wave length is often referred to as the dimensionless wave steepness, H/λ .

Since the distance between any two corresponding points on successive sine waves is the same, wave lengths and periods are usually actually measured between two consecutive upward (or downward) crossings of the still water level. Such points are also called zero-crossings, and are easier to detect in a wave record.

Since sine or cosine waves are expressed in terms of angular arguments, the wave length and period are converted to angles using:

$$\begin{aligned} k\lambda = 2\pi \quad \text{or:} \quad k &= \frac{2\pi}{\lambda} \\ \omega T = 2\pi \quad \text{or:} \quad \omega &= \frac{2\pi}{T} \end{aligned} \quad (4.1)$$

in which k is the wave number (rad/m) and ω is the circular wave frequency (rad/s).

Obviously, the wave form moves one wave length during one period so that its speed or phase velocity, c , is given by:

$$c = \frac{\lambda}{T} = \frac{\omega}{k} \quad (4.2)$$

If the wave moves in the positive x -direction, the wave profile - the form of the water surface - can now be expressed as a function of both x and t as follows:

$$\zeta = \zeta_a \cos(kx - \omega t) \quad (4.3)$$

Potential Theory

In order to use the potential linear theory, it will be necessary to assume that the water surface slope is very small. This means that the wave steepness is so small that terms in the equations of motion of the waves with a magnitude in the order of the steepness-squared can be ignored.

The profile of a simple wave with a small steepness looks like a sine or a cosine and the motion of a water particle in a wave depends on the distance below the still water level. This is reason why the wave potential is written as $\Phi_w(x, z, t) = P(z) \cdot \sin(kx - \omega t)$ in which $P(z)$ is a function of z .

This velocity potential $\Phi_w(x, z, t)$ of the harmonic waves has to fulfill four requirements:

1. Continuity condition or Laplace equation, which means that the fluid is homogeneous and incompressible.
2. Sea bed boundary condition, which means that the sea bed - at infinity here - is impervious.
3. Free surface dynamic boundary condition, which means that the pressure in the surface of the fluid is equal to the atmospheric pressure.
4. Free surface kinematic boundary condition, which means that a waterparticle in the surface of the fluid remains in that surface, the water surface is impervious too.

These requirements lead to a more complete expression for the velocity potential in deep water:

$$\Phi_w = \frac{-\zeta_a g}{\omega} \cdot e^{kz} \cdot \sin(\omega t - kx) \quad (4.4)$$

and the dispersion relation becomes:

$$\omega^2 = k g \quad (4.5)$$

Pressure

The pressure, p , in first order wave theory follows from the linearized Bernoulli equation:

$$\frac{\partial \Phi_w}{\partial t} + \frac{p}{\rho} + gz = 0 \quad \text{or:} \quad p = -\rho \frac{\partial \Phi_w}{\partial t} - \rho g z \quad (4.6)$$

With the wave potential the expression for the linearized dynamic part of the pressure in deep water becomes:

$$p_{dyn} = \rho g \zeta_a \cdot e^{kz} \cdot \cos(kx - \omega t) \quad (4.7)$$

Wave Energy

The energy in the waves consists of a potential and a kinetic part and the total wave energy can be written as:

$$E = \frac{1}{2} \rho g \zeta_a^2 \quad \text{per unit horizontal sea surface area} \quad (4.8)$$

4.2 Irregular Waves

Wind generated waves can be classified into two basic categories:

- **Sea**

A sea is a train of waves driven by the prevailing local wind field. The waves are short-crested with the lengths of the crests only a few (2-3) times the apparent wave length. Also, sea waves are very irregular; high waves are followed unpredictably by low waves and vice versa. Individual wave crests seem to propagate in different directions with tens of degrees deviation from the mean direction. The crests are fairly sharp and sometimes even small waves can be observed on these crests or there are dents in the larger wave crests or troughs. The apparent or virtual wave period, \tilde{T} , varies continuously, as well as the virtual or apparent wave length, $\tilde{\lambda}$.

- **Swell**

A swell is waves which have propagated out of the area and local wind in which they were generated. They are no longer dependent upon the wind and can even propagate for hundreds of kilometers through areas where the winds are calm. Individual waves are more regular and the crests are more rounded than those of a sea. The lengths of the crests are longer, now several (6-7) times the virtual wave length. The wave height is more predictable, too. If the swell is high, 5 to 6 waves of approximately

equal heights can pass a given point consecutively. If the waves are low, they can stay low for more than a minute even though the surface elevation remains irregular.

Wind waves, especially, are very irregular. Even so, they can be seen as a superposition of many simple, regular harmonic wave components, each with its own amplitude, length, period or frequency and direction of propagation. Such a concept can be very handy in many applications; it allows one to predict very complex irregular behavior in terms of much simpler theory of regular waves. This so-called **superposition principle**, first introduced in hydrodynamics by [St. Denis and Pierson, 1953], is illustrated in figure 4.2.

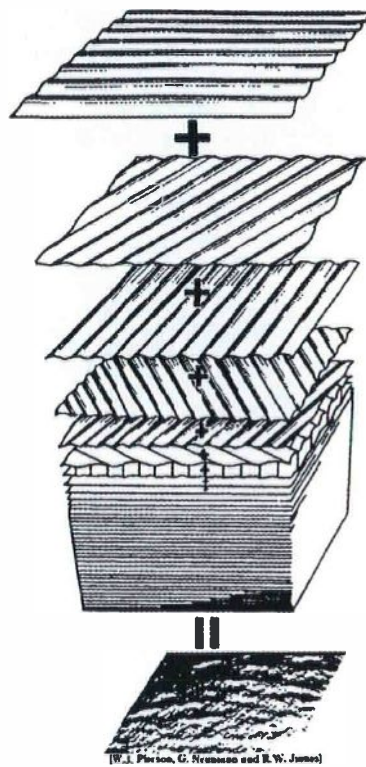


Figure 4.2: A Sum of Many Simple Sine Waves Makes an Irregular Sea

Energy Density Spectrum

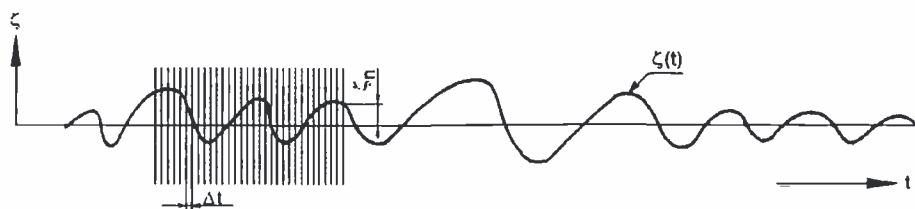


Figure 4.3: Registration and Sampling of a Wave

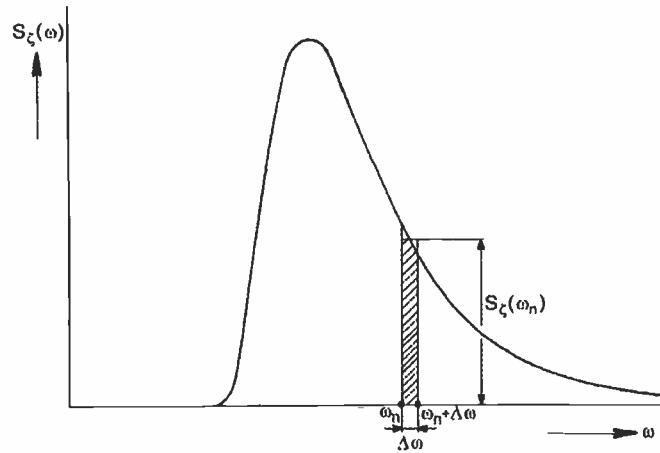


Figure 4.4: Definition of Spectral Density

Suppose a time history, as given in figure 4.3, of the wave elevation during a sufficient long but arbitrary period:

$$\tau = N \cdot \Delta t$$

The instantaneous wave elevation has a Gaussian distribution and zero mean.

The amplitudes ζ_{a_n} can be obtained by a Fourier analysis of the signal. However, for each little time shift of the time history one will find a new series of amplitudes ζ_{a_n} . Luckily, a mean square value of ζ_{a_n} can be found: $\overline{\zeta_{a_n}^2}$.

When $\zeta(t)$ is an irregular signal without prevailing frequencies, the average values $\overline{\zeta_{a_n}^2}$ close to ω_n will not change much as a function of the frequency; $\overline{\zeta_a^2}$ is a continuous function.

The variance σ_ζ^2 of this signal equals:

$$\begin{aligned} \sigma_\zeta^2 &= \overline{\zeta^2} \\ &= \frac{1}{N} \sum_{n=1}^N \zeta_n^2 = \frac{1}{N \cdot \Delta t} \sum_{n=1}^N \zeta_n^2 \cdot \Delta t \\ &= \frac{1}{\tau} \int_0^\tau \zeta^2(t) \cdot dt = \frac{1}{\tau} \int_0^\tau \left\{ \sum_{n=1}^N \zeta_{a_n} \cos(\omega_n t - k_n x + \varepsilon_n) \right\}^2 \cdot dt \\ &= \sum_{n=1}^N \frac{1}{2} \zeta_{a_n}^2 \end{aligned} \tag{4.9}$$

The wave amplitude ζ_{a_n} can be expressed by a wave spectrum $S_\zeta(\omega_n)$:

$$S_\zeta(\omega_n) \cdot \Delta\omega = \sum_{\omega_n}^{\omega_n + \Delta\omega} \frac{1}{2} \zeta_{a_n}^2(\omega) \tag{4.10}$$

where $\Delta\omega$ is a constant difference between two successive frequencies. Multiplied with ρg , this expression is the energy per unit area of the waves in the frequency interval $\Delta\omega$ see figure 4.4.

If m denotes a moment, then $m_{n\zeta}$ denotes the n^{th} order moment given in this case by:

$$m_{n\zeta} = \int_0^{\infty} \omega^n \cdot S_{\zeta}(\omega) \cdot d\omega \quad (4.13)$$

This means that $m_{0\zeta}$ is the area under the spectral curve, $m_{1\zeta}$ is the first order moment (static moment) of this area and $m_{2\zeta}$ is the second order moment (moment of inertia) of this area.

As has already been indicated, $m_{0\zeta}$ is an indication of the variance squared, σ_{ζ}^2 , of the water surface elevation. Of course this $m_{0\zeta}$ can also be related to the various wave amplitudes and heights:

$$\begin{aligned} \sigma_{\zeta} &= RMS = \sqrt{m_{0\zeta}} && \text{(Root Mean Square of the water surface elevation)} \\ \zeta_{a_{1/3}} &= 2 \cdot \sqrt{m_{0\zeta}} && \text{(significant wave amplitude)} \\ H_{1/3} &= 4 \cdot \sqrt{m_{0\zeta}} && \text{(significant wave height)} \end{aligned} \quad (4.14)$$

Characteristic wave periods can be defined from the spectral moments:

$$\begin{aligned} m_{1\zeta} &= \omega_1 \cdot m_{0\zeta} && \text{with } \omega_1 \text{ is spectral centroid} \\ m_{2\zeta} &= \omega_2^2 \cdot m_{0\zeta} && \text{with } \omega_2 \text{ is spectral radius of inertia} \end{aligned} \quad (4.15)$$

as follows:

$$\begin{aligned} T_1 &= 2\pi \cdot \frac{m_{0\zeta}}{m_{1\zeta}} && \text{(mean centroid wave period)} \\ T_2 &= 2\pi \cdot \sqrt{\frac{m_{0\zeta}}{m_{2\zeta}}} && \text{(mean zero-crossing wave period)} \end{aligned} \quad (4.16)$$

The mean zero-crossing period, T_2 , is sometimes indicated by T_z . One will often find the period associated with the peak of the spectrum, T_p , in the literature as well.

Rayleigh Distribution

Expressed in terms of $m_{0\zeta}$, the Rayleigh distribution is given by:

$$f(x) = \frac{x}{m_{0\zeta}} \cdot \exp\left\{-\frac{x^2}{2 \cdot m_{0\zeta}}\right\} \quad \text{(Rayleigh distribution)} \quad (4.17)$$

in which x is the variable being studied and $m_{0\zeta}$ is the area under the spectral curve. With this distribution, the probability that the wave amplitude, ζ_a , exceeds a chosen threshold value, a , can be calculated using:

$$\begin{aligned} P\{\zeta_a > a\} &= \int_a^{\infty} f(x) \cdot dx \\ &= \frac{1}{m_{0\zeta}} \int_a^{\infty} x \cdot \exp\left\{-\frac{x^2}{2 \cdot m_{0\zeta}}\right\} \cdot dx \\ &= \exp\left\{-\frac{a^2}{2 \cdot m_{0\zeta}}\right\} \end{aligned} \quad (4.18)$$

As an example, the probability that the wave height, H_w , in a certain sea state exceeds the significant wave height, $H_{1/3}$, is found by:

$$\begin{aligned} P \{H_w > H_{1/3}\} &= P \left\{ \zeta_a > \zeta_{a_{1/3}} \right\} \\ &= \exp \left\{ -\frac{\zeta_{a_{1/3}}^2}{2m_{0\zeta}} \right\} \\ &= e^{-2} \approx 0.135 \approx \frac{1}{7} \end{aligned} \quad (4.19)$$

Standard Wave Spectra

Investigators have attempted to describe a wave frequency spectrum in a standard form. Two important ones often found in the literature are described here. The mathematical formulations of these normalized uni-directional wave energy spectra are based on two parameters: the significant wave height, $H_{1/3}$, and average wave periods $\bar{T} = T_1, T_2$ or T_p :

$$S_\zeta(\omega) = H_{1/3}^2 \cdot f(\omega, \bar{T}) \quad (4.20)$$

Note that this definition means that the spectral values are proportional to the significant wave height squared; in other words $S_\zeta(\omega)/H_{1/3}^2$ is a function of ω and \bar{T} only.

Bretschneider Wave Spectra One of the oldest and most popular wave spectra was given by Bretschneider. It is especially suited for open sea areas. It is given mathematically by:

$$S_\zeta(\omega) = \frac{173 \cdot H_{1/3}^2}{T_1^4} \cdot \omega^{-5} \cdot \exp \left\{ \frac{-692}{T_1^4} \cdot \omega^{-4} \right\} \quad (4.21)$$

JONSWAP Wave Spectra In 1968 and 1969 an extensive wave measurement program, known as the Joint North Sea Wave Project (JONSWAP) was carried out along a line extending over 100 miles into the North Sea from Sylt Island. Analysis of the data yielded a spectral formulation for fetch-limited wind generated seas.

The following definition of a Mean JONSWAP wave spectrum is advised by the 17th ITTC in 1984 for fetch limited situations:

$$S_\zeta(\omega) = \frac{320 \cdot H_{1/3}^2}{T_p^4} \cdot \omega^{-5} \cdot \exp \left\{ \frac{-1950}{T_p^4} \cdot \omega^{-4} \right\} \cdot \gamma^A \quad (4.22)$$

with:

$$\gamma = 3.3 \quad (\text{peakedness factor})$$

$$A = \exp \left\{ -\left(\frac{\frac{\omega}{\omega_p} - 1}{\sigma\sqrt{2}} \right)^2 \right\}$$

$$\omega_p = \frac{2\pi}{T_p} \quad (\text{circular frequency at spectral peak})$$

$$\sigma = \begin{cases} 0.07 & \text{if } \omega < \omega_p \\ 0.09 & \text{if } \omega > \omega_p \end{cases}$$

Taking $\gamma^4 = 1.522$ results in the formulation of the Bretschneider wave spectrum with the peak period T_p . Sometimes, a third free parameter is introduced in the JONSWAP wave spectrum by varying the peakedness factor γ .

Wave Spectra Comparison Figure 4.6 compares the Bretschneider and mean JONSWAP wave spectra for three sea states with a significant wave height, $H_{1/3}$, of 4 meters and peak periods, T_p , of 6, 8 and 10 seconds, respectively. The figure shows the more pronounced peak of the JONSWAP spectrum.

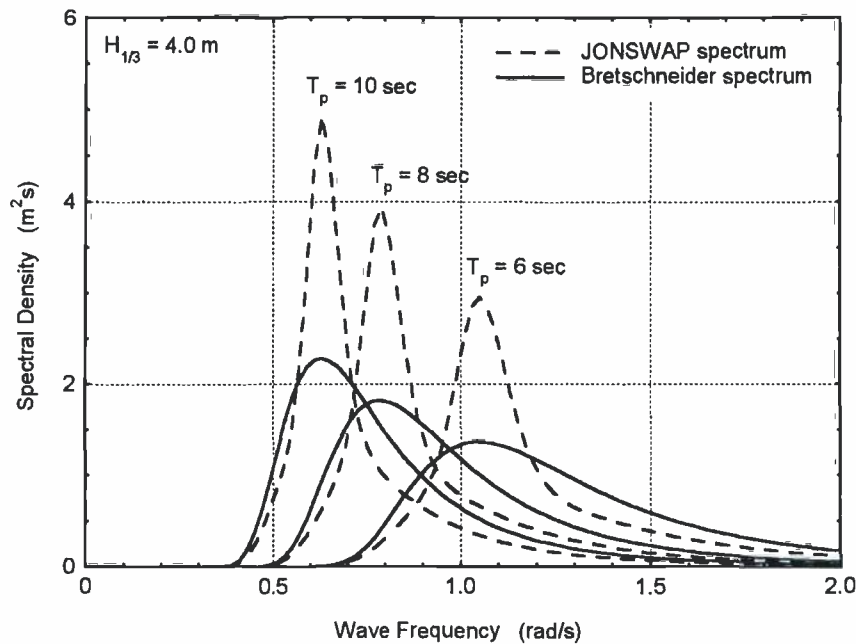


Figure 4.6: Comparison of Two Spectral Formulations

Wave Prediction and Climatology

In 1805, the British Admiral Sir Francis Beaufort devised an observation scale for measuring winds at sea. His scale measures winds by observing their effects on sailing ships and waves and is still used today by many weather stations. A definition of this Beaufort wind force scale is given in figure 4.7. The pictures in figure 4.8 give a visual impression of the sea states in relation to Beaufort's scale.

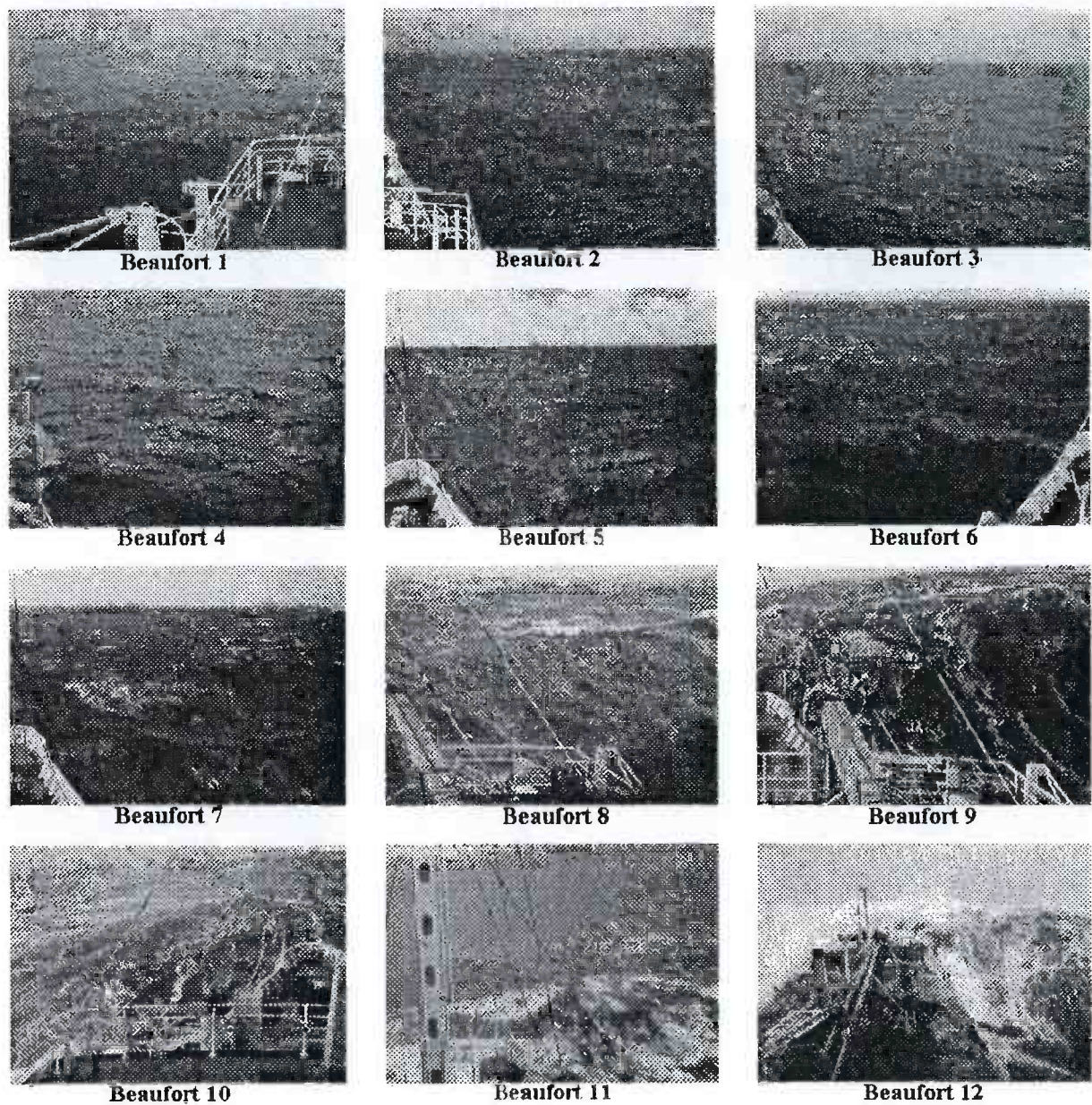


Figure 4.8: Sea State in Relation to Beaufort Wind Force Scale

Storm Wave Data

An entire storm can be characterized by just two numbers: one related to the wave period and one to the wave height. It now becomes important to predict these values from other data - such as geographical and meteorological information. Figure 4.9 for "Open Ocean Areas" and "North Sea Areas" gives an indication of an average relationship between the Beaufort wind scale and the significant wave height $H_{1/3}$ and the average wave periods T_1 and T_2 , defined before.

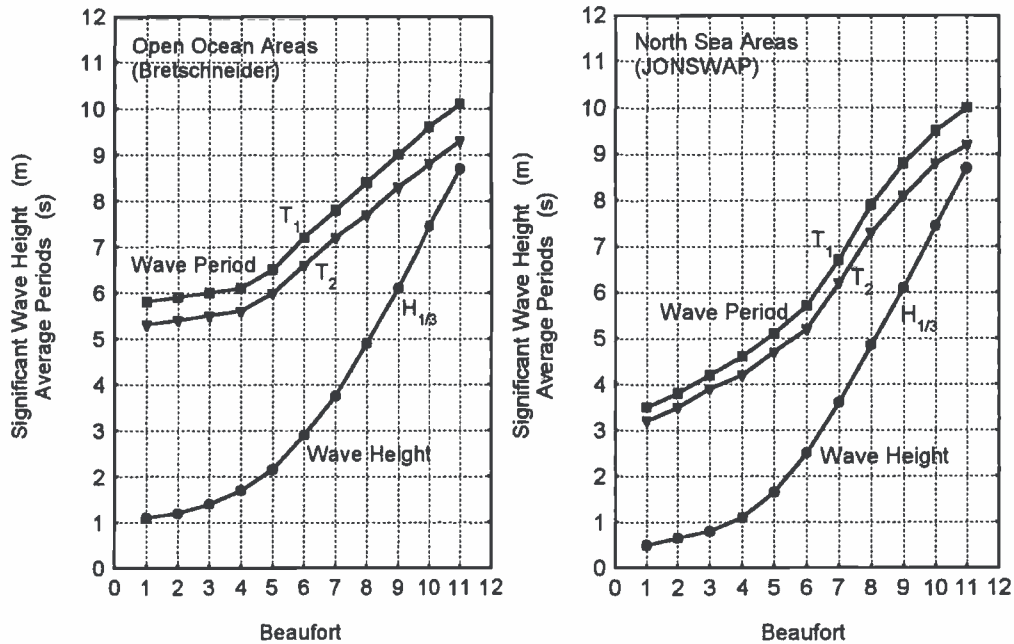


Figure 4.9: Wave Spectrum Parameter Estimates

Long Term Wave Data

Longer term wave climatology is used to predict the statistical chance that a given wave-sensitive offshore operation - such as lifting a major topside element into place - will be delayed by sea conditions which are too rough. Sets of characteristic wave data values can be grouped and arranged in a table such as that given below for all wave directions in the winter season in areas 8, 9, 15 and 16 of the North Atlantic Ocean. A 'storm' here is an arbitrary time period - often of 3 or 6 hours - for which a single pair of values has been collected. The number in each cell of this table indicates the chance that a significant wave height is between the values in the left column and in the range of wave periods listed at the top of the table.

Winter Data of Areas 8, 9, 15 and 16 of the North Atlantic (Global Wave Statistics)											
	T ₂ (s)										
H _s (m)	3.5	4.5	5.5	6.5	7.5	8.5	9.5	10.5	11.5	12.5	13.5
14.5	0	0	0	0	2	30	154	362	466	370	202
13.5	0	0	0	0	3	33	145	293	322	219	101
12.5	0	0	0	0	7	72	289	539	548	345	149
11.5	0	0	0	0	17	160	585	996	931	543	217
10.5	0	0	0	1	41	363	1200	1852	1579	843	310
9.5	0	0	0	4	109	845	2485	3443	2648	1283	432
8.5	0	0	0	12	295	1996	5157	6323	4333	1882	572
7.5	0	0	0	41	818	4723	10537	11242	6755	2594	703
6.5	0	0	1	138	2273	10967	20620	18718	9665	3222	767
5.5	0	0	7	471	6187	24075	36940	27702	11969	3387	694
4.5	0	0	31	1586	15757	47072	56347	33539	11710	2731	471
3.5	0	0	148	5017	34720	74007	64809	28964	7804	1444	202
2.5	0	4	681	13441	56847	77259	46013	13962	2725	381	41
1.5	0	40	2699	23284	47839	34532	11554	2208	282	27	2
0.5	5	350	3314	8131	5858	1598	216	18	1	0	0

Chapter 5

Behavior of Structures in Waves

The dynamics of rigid bodies and fluid motions are governed by the combined actions of different external forces and moments as well as by the inertia of the bodies themselves. In fluid dynamics these forces and moments can no longer be considered as acting at a single point or at discrete points of the system. Instead, they must be distributed in a relatively smooth or a continuous manner throughout the mass of the fluid particles. The force and moment distributions and the kinematic description of the fluid motions are in fact continuous, assuming that the collection of discrete fluid molecules can be analyzed as a continuum.

5.1 Behavior in Regular Waves

When a ship moves with a forward speed in waves with a frequency ω and a wave direction μ , the frequency at which it encounters the waves, ω_e , becomes important. The relation between the frequency of encounter and the wave frequency becomes:

$$\omega_e = \omega - kV \cos \mu \quad (5.1)$$

Note that $\mu = 0$ for following waves.

Motions of and about CoG

The ship motions in the steadily translating $O(x, y, z)$ system are defined by three translations of the ship's center of gravity (CoG) in the direction of the x -, y - and z -axes and three rotations about them as given in figure 5.1:

$$\begin{aligned} \text{Surge} & : & x & = x_a \cos(\omega_e t + \varepsilon_{x\zeta}) \\ \text{Sway} & : & y & = y_a \cos(\omega_e t + \varepsilon_{y\zeta}) \\ \text{Heave} & : & z & = z_a \cos(\omega_e t + \varepsilon_{z\zeta}) \\ \text{Roll} & : & \phi & = \phi_a \cos(\omega_e t + \varepsilon_{\phi\zeta}) \\ \text{Pitch} & : & \theta & = \theta_a \cos(\omega_e t + \varepsilon_{\theta\zeta}) \\ \text{Yaw} & : & \psi & = \psi_a \cos(\omega_e t + \varepsilon_{\psi\zeta}) \end{aligned} \quad (5.2)$$

in which each of the ε values is a different phase angle.

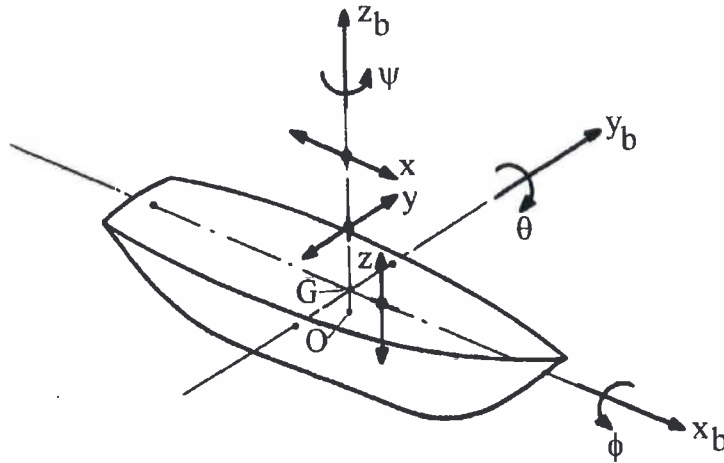


Figure 5.1: Definition of Ship Motions in Six Degrees of Freedom

Knowing the motions of and about the center of gravity, G , one can calculate the motions in any point on the structure using superposition.

The phase shifts of these motions are related to the harmonic wave elevation at the origin of the steadily translating $O(x, y, z)$ system, the average position of the ship's center of gravity - even though no wave can be measured there:

$$\text{Wave elevation at } O \text{ or } G: \quad \zeta = \zeta_a \cos(\omega_e t) \tag{5.3}$$

Displacement, Velocity and Acceleration

The harmonic velocities and accelerations in the steadily translating $O(x, y, z)$ coordinate system are found by taking the derivatives of the displacements.

For roll:

$$\begin{aligned} \text{Displacement} & : \quad \phi = \phi_a \cos(\omega_e t + \varepsilon_{\phi\zeta}) \\ \text{Velocity} & : \quad \dot{\phi} = -\omega_e \phi_a \sin(\omega_e t + \varepsilon_{\phi\zeta}) = \omega_e \phi_a \cos(\omega_e t + \varepsilon_{\phi\zeta} - \pi/2) \\ \text{Acceleration} & : \quad \ddot{\phi} = -\omega_e^2 \phi_a \cos(\omega_e t + \varepsilon_{\phi\zeta}) = \omega_e^2 \phi_a \cos(\omega_e t + \varepsilon_{\phi\zeta} - \pi) \end{aligned} \tag{5.4}$$

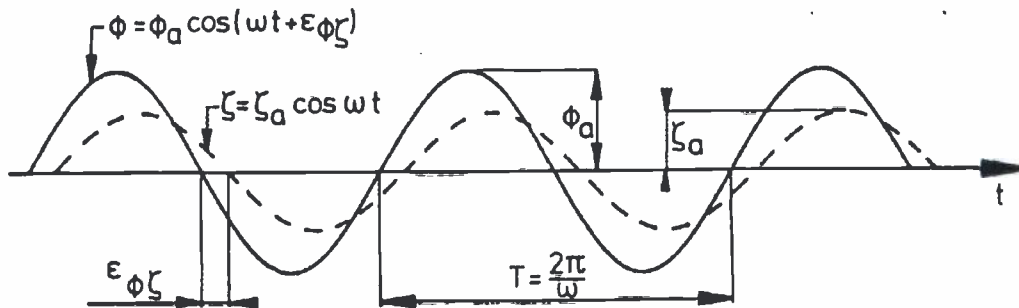


Figure 5.2: Harmonic Wave and Roll Signal

The phase shift of the roll motion with respect to the wave elevation, $\varepsilon_{\phi\zeta}$ in figure 5.2, is positive, here because when the wave elevation passes zero at a certain instant, the roll motion already has passed zero. Thus, if the roll motion, ϕ , comes before the wave elevation, ζ , then the phase shift, $\varepsilon_{\phi\zeta}$, is defined as positive. This convention will hold for all other responses as well of course.

Figure 5.3 shows a sketch of the time histories of the harmonic angular displacements, velocities and accelerations of roll. Note the mutual phase shifts of $\pi/2$ and π .

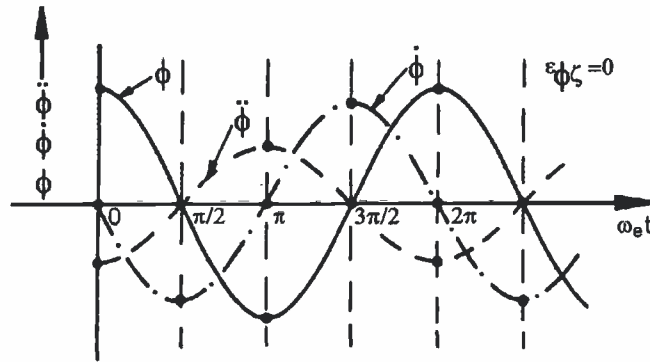


Figure 5.3: Displacement, Acceleration and Velocity

5.1.1 Equations of Motion

Consider a seaway with irregular waves of which the energy distribution over the wave frequencies (the wave spectrum) is known. These waves are input to a system that possesses linear characteristics. These frequency characteristics are known, for instance via model experiments or computations. The output of the system is the motion of the floating structure. This motion has an irregular behavior, just as the seaway that causes the motion. The block diagram of this principle is given in figure 5.4.

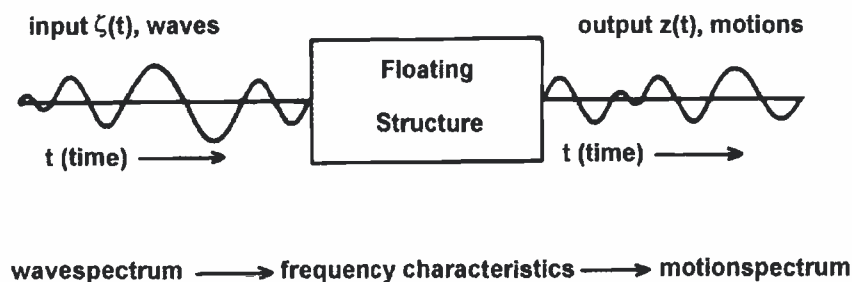


Figure 5.4: Relation between Motions and Waves

The first harmonics of the motion components of a floating structure are often of interest, because in many cases a very realistic mathematical model of the motions in a seaway can be obtained by making use of a superposition of these components at each of a range of frequencies; motions in the so-called frequency domain will be considered here.

In many cases the ship motions have mainly a linear behavior. This means that, at each frequency, the ratios between the motion amplitudes and the wave amplitudes and also the phase shifts between the motions and the waves are constant. Doubling the input (wave) amplitude results in a doubled output amplitude, while the phase shifts between output and input does not change.

As a consequence of the linear theory, the resulting motions in irregular waves can be obtained by adding together results from regular waves of different amplitudes, frequencies and possibly propagation directions. With known wave energy spectra and the calculated frequency characteristics of the responses of the ship, the response spectra and the statistics of these responses can be found.

Kinetics

A rigid body's equation of motions with respect to an earth-bound coordinate system follow from Newton's second law. The vector equations for the translations of and the rotations about the center of gravity are respectively given by:

$$\vec{F} = \frac{d}{dt} (m\vec{U}) \quad \text{and} \quad \vec{M} = \frac{d}{dt} (\vec{H}) \quad (5.5)$$

in which \vec{F} is the resulting external force acting in the center of gravity (N), m is the mass of the rigid body (kg), \vec{U} is the instantaneous velocity of the center of gravity (m/s), \vec{M} is the resulting external moment acting about the center of gravity (Nm), \vec{H} is the instantaneous angular momentum about the center of gravity (Nms) and t is the time (s). The total mass as well as its distribution over the body is considered to be constant during a time which is long relative to the oscillation period of the motions.

Loads Superposition

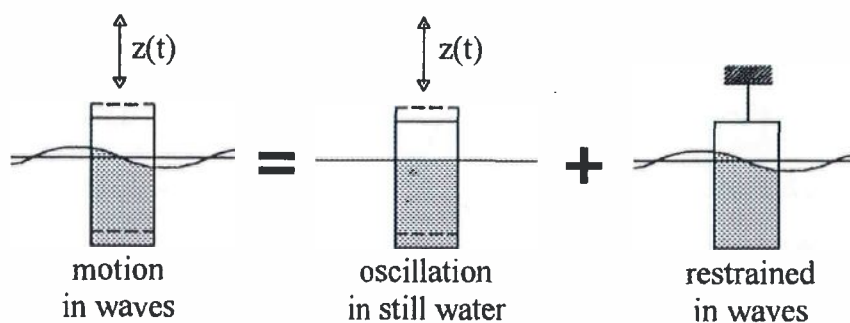


Figure 5.5: Superposition of Hydromechanical and Wave Loads

Since the system is linear, the resulting motion in waves can be seen as a superposition of the motion of the body in still water and the forces on the restrained body in waves. Thus, two important assumptions are made here for the loads on the right hand side of the picture equation in figure 5.5:

- a. The so-called **hydromechanical forces and moments** are induced by the harmonic oscillations of the rigid body, moving in the undisturbed surface of the fluid.

- b. The so-called **wave exciting forces and moments** are produced by waves coming in on the restrained body.

The vertical motion of the body follows from:

$$\frac{d}{dt} (\rho \nabla \cdot \dot{z}) = \rho \nabla \cdot \ddot{z} = F_h + F_w \tag{5.6}$$

in which ρ is the density of water (kg/m^3), ∇ is the volume of displacement of the body (m^3), F_h is the hydromechanical force in the z -direction (N) and F_w is the exciting wave force in the z -direction (N).

This superposition will be explained in more detail for a circular cylinder, floating in still water with its center line in the vertical direction, as shown in figure 5.6.

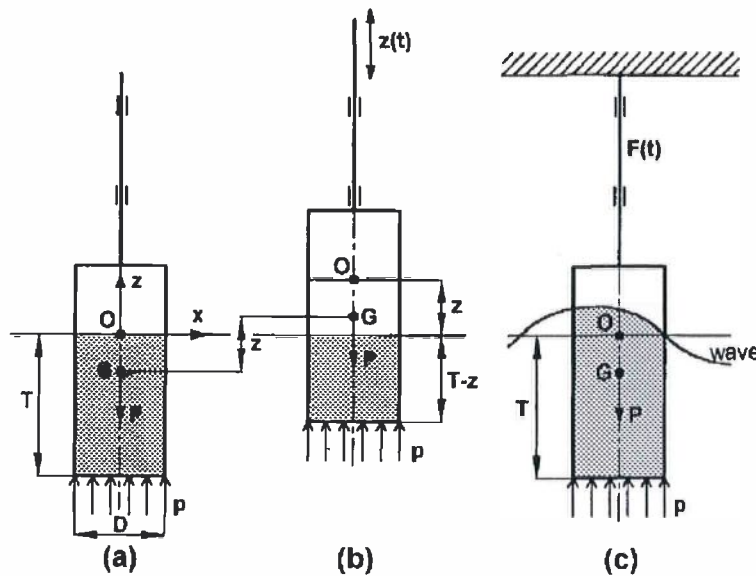


Figure 5.6: Heaving Circular Cylinder

Hydromechanical Loads

First, a free decay test in still water will be considered. After a vertical displacement upwards (see 5.6-b), the cylinder will be released and the motions can die out freely. The vertical motions of the cylinder are determined by the solid mass m of the cylinder and the hydromechanical loads on the cylinder.

Applying Newton's second law for the heaving cylinder:

$$\begin{aligned} m\ddot{z} &= \text{sum of all forces on the cylinder} \\ &= -P + pA_w - b\dot{z} - a\ddot{z} \\ &= -P + \rho g (T - z) A_w - b\dot{z} - a\ddot{z} \end{aligned} \tag{5.7}$$

With Archimedes' law $P = \rho g T A_w$, the linear equation of the heave motion becomes:

$$(m + a) \ddot{z} + b\dot{z} + cz = 0 \tag{5.8}$$

in which z is the vertical displacement (m), $P = mg$ is the mass force downwards (N), $m = \rho A_w T$ is the solid mass of cylinder (kg), a is the hydrodynamic mass coefficient ($\text{Ns}^2/\text{m} = \text{kg}$), b is the hydrodynamic damping coefficient ($\text{Ns}/\text{m} = \text{kg}/\text{s}$), $c = \rho g A_w$ is the restoring spring coefficient ($\text{N}/\text{m} = \text{kg}/\text{s}^2$), $A_w = \frac{\pi}{4} D^2$ is the water plane area (m^2), D is the diameter of the cylinder (m) and T is the draft of the cylinder at rest (s).

The terms $a\ddot{z}$ and $b\dot{z}$ are caused by the hydrodynamic reaction as a result of the movement of the cylinder with respect to the water. The water is assumed to be ideal and thus to behave as in a potential flow.

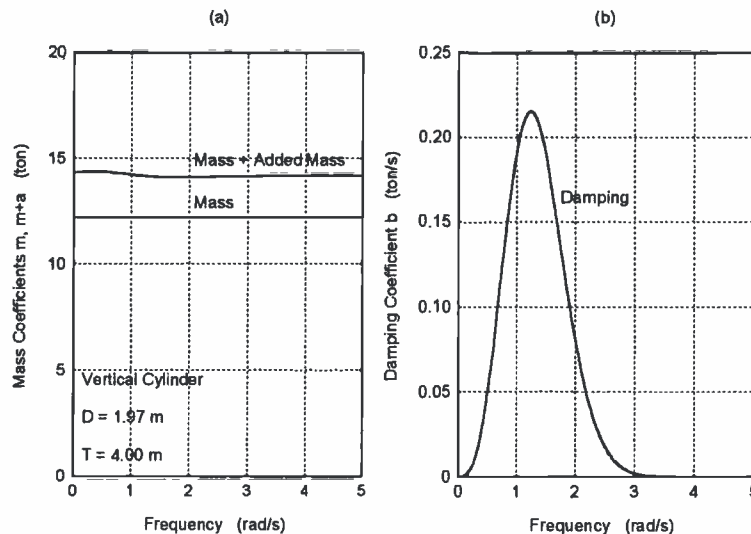


Figure 5.7: Mass and Damping of a Heaving Vertical Cylinder

The vertical oscillations of the cylinder will generate waves which propagate radially from it. Since these waves transport energy, they withdraw energy from the (free) buoy's oscillations; its motion will die out. This so-called wave damping is proportional to the velocity of the cylinder \dot{z} in a linear system. The coefficient b has the dimension of a mass per unit of time and is called the **(wave or potential) damping** coefficient. Figure 5.7-b shows the hydrodynamic damping coefficient b of a vertical cylinder as a function of the frequency of oscillation. In an actual viscous fluid, friction also causes damping, vortices and separation phenomena. Generally, these viscous contributions to the damping are non-linear, but they are usually small for most large floating structures; they are neglected here for now.

The other part of the hydromechanical reaction force $a\ddot{z}$ is proportional to the vertical acceleration of the cylinder in a linear system. This force is caused by accelerations that are given to the water particles near to the cylinder. This part of the force does not dissipate energy and manifests itself as a standing wave system near the cylinder. The coefficient a has the dimension of a mass and is called the **hydrodynamic mass** or **added mass**. Figure 5.7-a shows the hydrodynamic mass a of a vertical cylinder as a function of the frequency of oscillation.

It appears from experiments that in many cases both the acceleration and the velocity terms have a sufficiently linear behavior at small amplitudes; they are linear for practical purposes. The hydromechanical forces are the total reaction forces of the fluid on the

oscillating cylinder, caused by this motion in initially still water:

$$m\ddot{z} = F_h \quad \text{with: } F_h = -a\ddot{z} - b\dot{z} - cz \quad (5.9)$$

and the equation of motion of the decaying cylinder in still water becomes:

$$(m + a) \cdot \ddot{z} + b \cdot \dot{z} + c \cdot z = 0 \quad (5.10)$$

Wave Loads

Waves are now generated in the test basin for a new series of tests. The object is restrained so that one now measures (in this vertical cylinder example) the vertical wave load on the fixed cylinder. This is shown schematically in figure 5.6-c.

The classic theory of deep water waves yields:

$$\begin{aligned} \text{wave potential : } \quad \Phi &= \frac{-\zeta_a g}{\omega} e^{kz} \sin(\omega t - kx) \\ \text{wave elevation : } \quad \zeta &= \zeta_a \cos(\omega t - kx) \end{aligned} \quad (5.11)$$

so that the pressure, p , on the bottom of the cylinder ($z = -T$) follows from the linearized Bernoulli equation:

$$\begin{aligned} p &= -\rho \frac{\partial \Phi}{\partial t} - \rho g z \\ &= \rho g \zeta_a e^{kz} \cos(\omega t - kx) - \rho g z \\ &= \rho g \zeta_a e^{-kT} \cos(\omega t - kx) + \rho g T \end{aligned} \quad (5.12)$$

Assuming that the diameter of the cylinder is small relative to the wave length ($kD \approx 0$), so that the pressure distribution on the bottom of the cylinder is essentially uniform, then the pressure becomes:

$$p = \rho g \zeta_a e^{-kT} \cos(\omega t) + \rho g T \quad (5.13)$$

Then the vertical force on the bottom of the cylinder is:

$$F = \{ \rho g \zeta_a e^{-kT} \cos(\omega t) + \rho g T \} \cdot \frac{\pi}{4} D^2 \quad (5.14)$$

where D is the cylinder diameter and T is the draft.

The harmonic part of this force is the regular harmonic wave force, which will be considered here. More or less in the same way as with the hydromechanical loads (on the oscillating body in still water), this wave force can also be expressed as a spring coefficient c times a reduced or effective wave elevation ζ^* :

$$\begin{aligned} F_{FK} &= c \cdot \zeta^* \quad \text{with: } c = \rho g \frac{\pi}{4} D^2 \quad (\text{spring coeff.}) \\ \zeta^* &= e^{-kT} \cdot \zeta_a \cos(\omega t) \quad (\text{deep water}) \end{aligned} \quad (5.15)$$

This wave force is called the **Froude-Krilov force**, which follows from an integration of the pressures on the body in the undisturbed wave.

Actually however, a part of the waves will be diffracted, requiring a correction of this Froude-Krilov force. Using the relative motion principle described earlier in this chapter,

one finds additional force components: one proportional to the vertical acceleration of the water particles and one proportional to the vertical velocity of the water particles. The total wave force can be written as:

$$F_w = a\ddot{\zeta}^* + b\dot{\zeta}^* + c\zeta^* = F_a \cos(\omega t + \varepsilon_{F\zeta}) \quad (5.16)$$

in which the terms $a\ddot{\zeta}^*$ and $b\dot{\zeta}^*$ are considered to be corrections on the Froude-Krilov force due to diffraction of the waves by the presence of the cylinder in the fluid. The "reduced" wave elevation is given by:

$$\begin{aligned} \zeta^* &= \zeta_a e^{-kT} \cos(\omega t) \\ \dot{\zeta}^* &= -\zeta_a e^{-kT} \omega \sin(\omega t) \\ \ddot{\zeta}^* &= -\zeta_a e^{-kT} \omega^2 \cos(\omega t) \end{aligned} \quad (5.17)$$

The wave force amplitude, F_a , is proportional to the wave amplitude, ζ_a , and the phase shift $\varepsilon_{F\zeta}$ is independent of the wave amplitude, ζ_a ; the system is linear.

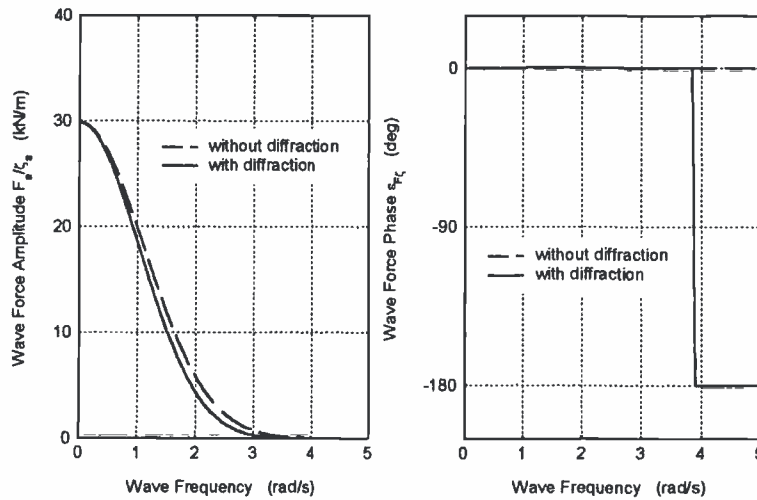


Figure 5.8: Vertical Wave Force on a Vertical Cylinder

Figure 5.8 shows the wave force amplitude and phase shift as a function of the wave frequency. For low frequencies (long waves), the diffraction part is very small and the wave force tends to the Froude-Krilov force, $c\zeta^*$. At higher frequencies there is a small influence of diffraction on the wave force on this vertical cylinder. There, the wave force amplitude remains almost similar to the Froude-Krilov force. Diffraction becomes relatively important after the total force has become small; an abrupt phase shift of $-\pi$ occurs quite suddenly, too.

Equation of Motion

The addition of the exciting wave loads from equation 5.16 to the right hand side of equation 5.8, gives the equation of motion for this heaving cylinder in waves:

$$(m + a)\ddot{z} + b\dot{z} + cz = a\ddot{\zeta}^* + b\dot{\zeta}^* + c\zeta^* \quad (5.18)$$

The heave response to the regular wave excitation is given by:

$$\begin{aligned} z &= z_a \cos(\omega t + \varepsilon_{z\zeta}) \\ \dot{z} &= -z_a \omega \sin(\omega t + \varepsilon_{z\zeta}) \\ \ddot{z} &= -z_a \omega^2 \cos(\omega t + \varepsilon_{z\zeta}) \end{aligned} \tag{5.19}$$

Some algebra results in the heave amplitude:

$$\frac{z_a}{\zeta_a} = e^{-kT} \sqrt{\frac{\{c - a\omega^2\}^2 + \{b\omega\}^2}{\{c - (m + a)\omega^2\}^2 + \{b\omega\}^2}} \tag{5.20}$$

and the phase shift:

$$\varepsilon_{z\zeta} = \arctan \left\{ \frac{-mb\omega^3}{(c - a\omega^2) \{c - (m + a)\omega^2\} + \{b\omega\}^2} \right\} \quad \text{with : } 0 \leq \varepsilon_{z\zeta} \leq 2\pi \tag{5.21}$$

The requirements of linearity is fulfilled: the heave amplitude z_a is proportional to the wave amplitude ζ_a and the phase shift $\varepsilon_{z\zeta}$ is not dependent on the wave amplitude ζ_a .

5.1.2 Frequency Characteristics

Generally, the amplitudes and phase shifts in the previous section are called:

$$\left. \begin{aligned} \frac{F_a}{\zeta_a}(\omega) \text{ and } \frac{z_a}{\zeta_a}(\omega) &= \text{amplitude characteristics} \\ \varepsilon_{F\zeta}(\omega) \text{ and } \varepsilon_{z\zeta}(\omega) &= \text{phase characteristics} \end{aligned} \right\} \text{frequency characteristics}$$

The response amplitude characteristics $\frac{z_a}{\zeta_a}(\omega)$ are also referred to as **Response Amplitude Operator (RAO)**.

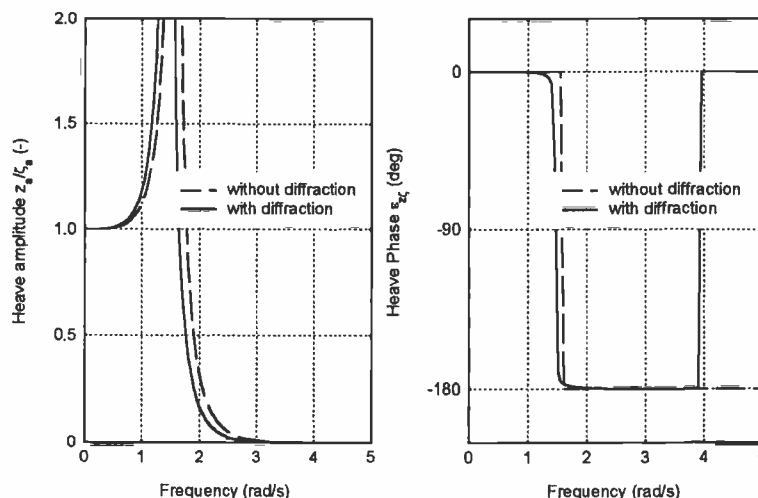


Figure 5.9: Heave Motions of a Vertical Cylinder

Figure 5.9 shows the frequency characteristics for heave together with the influence of diffraction of the waves. The annotation "without diffraction" in these figures means that the wave load consists of the Froude-Krilov force, $c\zeta^*$, only. A phase shift of $-\pi$ occurs at

the natural frequency. This phase shift is very abrupt here, because of the small damping of this cylinder. A second phase shift appears at a higher frequency. This is caused by a phase shift in the wave load.

Equation 5.20 and figure 5.10 show that with respect to the motional behavior of this cylinder three frequency areas can be distinguished:

- the low frequency area ($\omega^2 \ll c/(m+a)$), with motions dominated by the restoring spring term,
- the natural frequency area ($c/(m+a) \lesssim \omega^2 \lesssim c/a$), with motions dominated by the damping term and
- the high frequency area ($\omega^2 \gg c/a$), with motions dominated by the mass term.

Also, equation 5.20 shows that the vertical motion tends to the wave motion as the frequency decreases to zero.

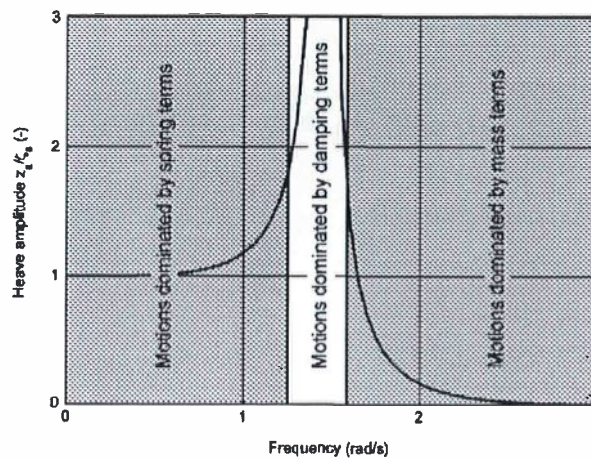


Figure 5.10: Frequency Areas with Respect to Motional Behavior

Figure 5.11 shows the speed dependent transfer functions of the roll motions in beam waves and the pitch motions in head waves of a container ship. Notice the opposite effect of forward speed on these two angular motions, caused by a with forward speed strongly increasing lift-damping of the roll motions.

Figure 5.12 shows the speed dependent transfer functions of the absolute and the relative vertical bow motions of a container ship in head waves. Note the opposite characteristics of these two motions in very short and in very long waves.

The resonance frequency of a motion does not necessarily coincides with the natural frequency. A clear example of this is given by [Hooft, 1970], as shown in figure 5.13, for a semi-submersible platform with different dimensions of the under water geometry. This geometry has been configured in such a way that the responses are minimal at the natural frequency.

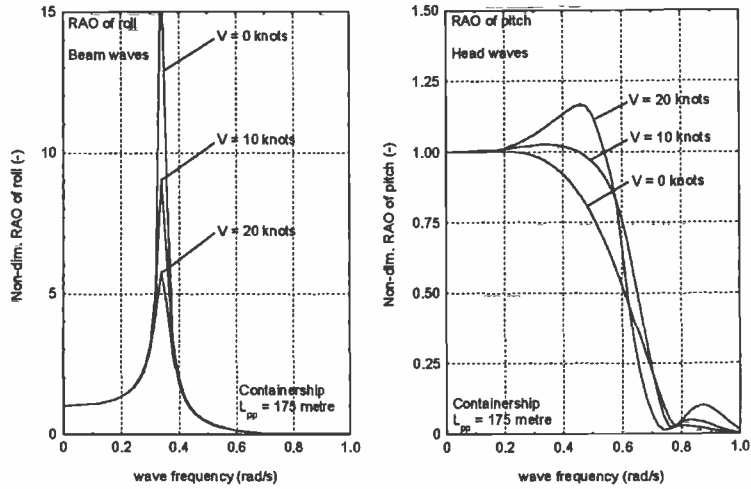


Figure 5.11: RAO's of Roll and Pitch of a Containership

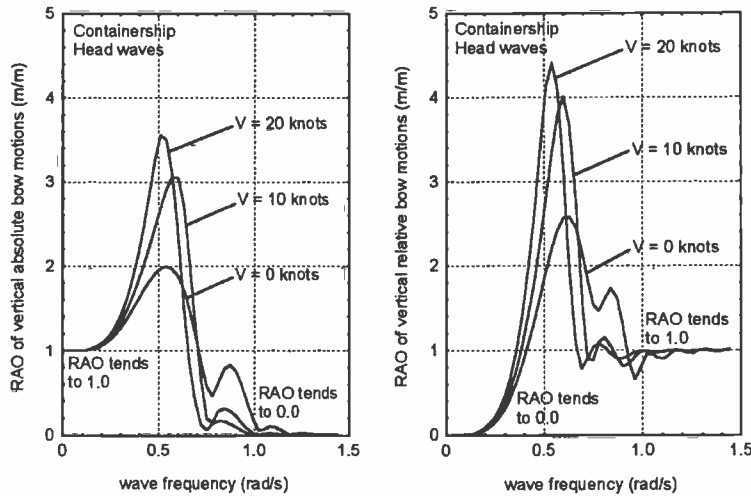


Figure 5.12: Absolute and Relative Vertical Motions at the Bow

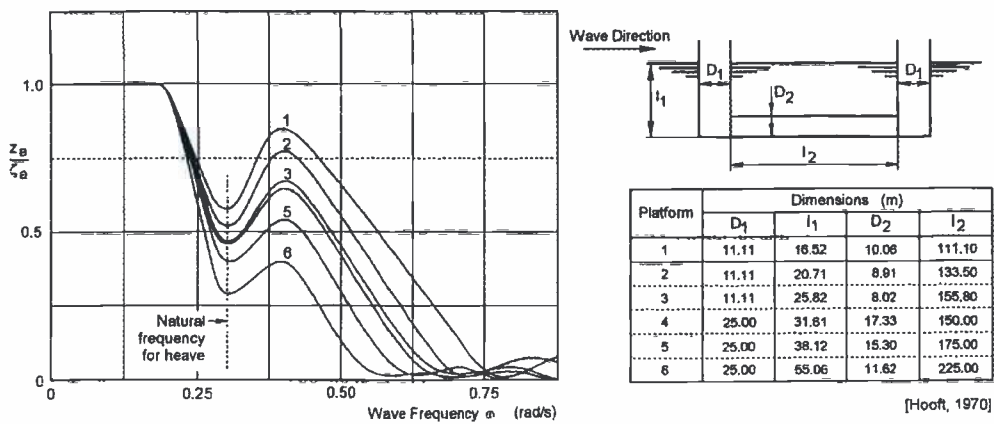


Figure 5.13: Heave Responses of Semi-Submersible Platforms in Waves

5.2 Behavior in Irregular Waves

When information on the irregular waves is available, now first as well as second order motions can be determined.

5.2.1 First Order Motions

The wave energy spectrum was defined by:

$$S_{\zeta}(\omega) \cdot d\omega = \frac{1}{2} \zeta_a^2(\omega) \quad (5.22)$$

Analogous to this, the energy spectrum of the heave response $z(\omega, t)$ can be defined by:

$$\begin{aligned} S_z(\omega) \cdot d\omega &= \frac{1}{2} z_a^2(\omega) \\ &= \left| \frac{z_a}{\zeta_a}(\omega) \right|^2 \cdot \frac{1}{2} \zeta_a^2(\omega) \\ &= \left| \frac{z_a}{\zeta_a}(\omega) \right|^2 \cdot S_{\zeta}(\omega) \cdot d\omega \end{aligned} \quad (5.23)$$

Thus, the heave response spectrum of a motion can be found by using the transfer function of the motion and the wave spectrum by:

$$S_z(\omega) = \left| \frac{z_a}{\zeta_a}(\omega) \right|^2 \cdot S_{\zeta}(\omega) \quad (5.24)$$

The principle of this transformation of wave energy to response energy is shown in figure 5.14 for the heave motions being considered here.

The irregular wave history, $\zeta(t)$ - below in the left hand side of the figure - is the sum of a large number of regular wave components, each with its own frequency, amplitude and a random phase shift. The value $\frac{1}{2} \zeta_a^2(\omega) / \Delta\omega$ - associated with each wave component on the ω -axis - is plotted vertically on the left; this is the wave energy spectrum, $S_{\zeta}(\omega)$. This part of the figure can be found in chapter 5 as well, by the way.

Each regular wave component can be transferred to a regular heave component by a multiplication with the transfer function $z_a / \zeta_a(\omega)$. The result is given in the right hand side of this figure. The irregular heave history, $z(t)$, is obtained by adding up the regular heave components, just as was done for the waves on the left. Plotting the value $\frac{1}{2} z_a^2(\omega) / \Delta\omega$ of each heave component on the ω -axis on the right yields the heave response spectrum, $S_z(\omega)$.

The moments of the heave response spectrum are given by:

$$m_{nz} = \int_0^{\infty} S_z(\omega) \cdot \omega^n \cdot d\omega \quad \text{with: } n = 0, 1, 2, \dots \quad (5.25)$$

where $n = 0$ provides the area, $n = 1$ the first moment and $n = 2$ the moment of inertia of the spectral curve.

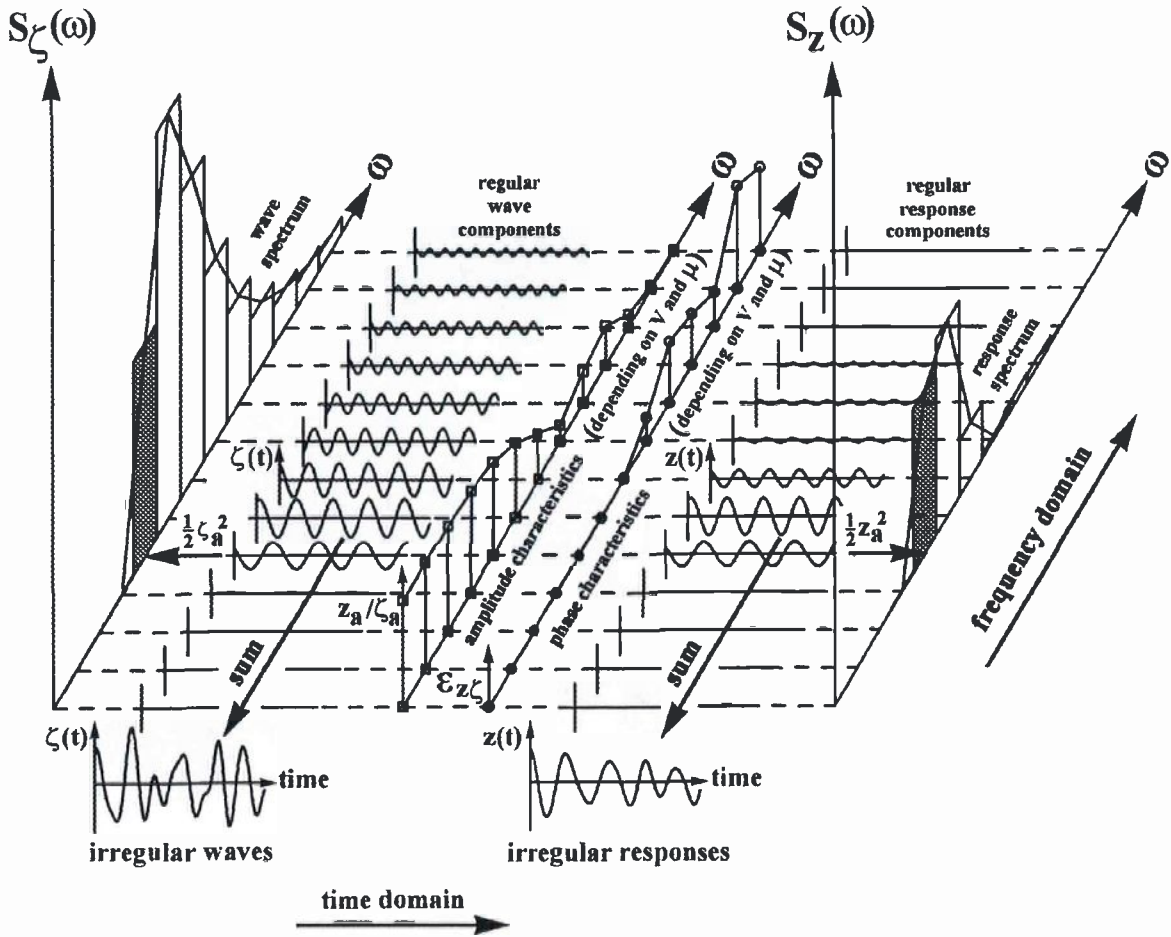


Figure 5.14: Principle of Transfer of Waves into Responses

The significant heave amplitude can be calculated from the spectral density function of the heave motions, just as was done for waves. This significant heave amplitude, defined as the mean value of the highest one-third part of the amplitudes, is:

$$\bar{z}_{a1/3} = 2 \cdot RMS = 2 \cdot \sqrt{m_{0z}} \tag{5.26}$$

in which $RMS (= \sqrt{m_{0z}})$ is the Root Mean Square value.

A mean period, T_{1z} , can be found from the centroid of the spectrum or a period, T_{2z} , equivalent to the average zero-crossing period, found from the spectral radius of gyration:

$$T_{1z} = 2\pi \cdot \frac{m_{0z}}{m_{1z}} \quad \text{and} \quad T_{2z} = 2\pi \cdot \sqrt{\frac{m_{0z}}{m_{2z}}} \tag{5.27}$$

Figure 5.15 shows an example of the striking influence of the average wave period on a response spectrum. This response is the heave motion of a 175 meter container ship, sailing with a speed of 20 knots in head waves with a significant wave height of 5.0 meters. For the wave spectrum with an average period of 6.0 seconds, the transfer function has very low values in the wave frequency range. The response spectrum becomes small; only small motions result. As the average wave period gets larger (to the right in figure 5.15), the response increases dramatically.

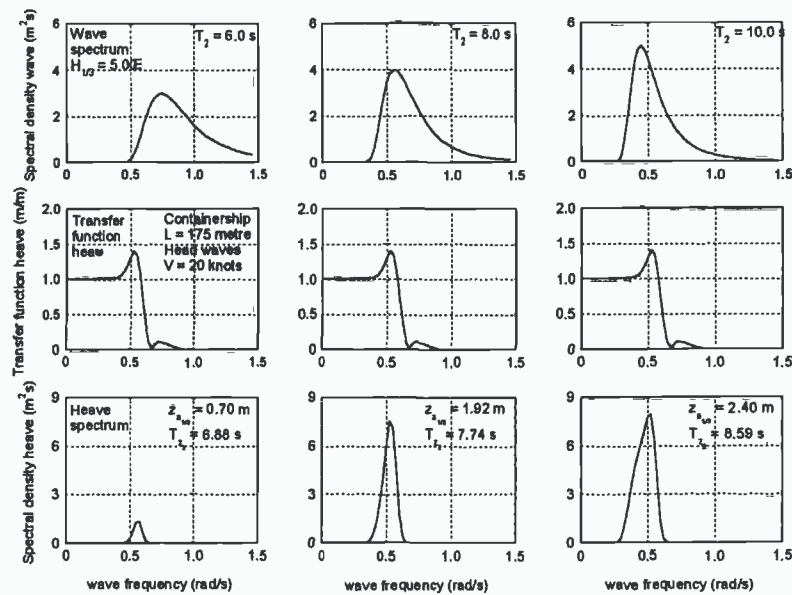


Figure 5.15: Effect of Wave Period on Heave

A similar effect will be obtained for a larger range of average wave periods if the transfer function of the motion shifts to the low frequency region. A low natural frequency is required to obtain this. This principle has been used when designing semi-submersibles, which have a large volume under water and a very small spring term for heave (small water plane area). However, such a shape does not make much of a wave when it oscillates; it has little potential damping. This results in large (sometimes very large) *RAO*'s at the natural frequency. As long as there is (almost) no wave energy at this frequency, the response spectrum will remain small.

Figure 5.16 shows a wave spectrum with sketches of *RAO*'s for heave of three different types of floating structures at zero forward speed:

- The pontoon has a relatively large natural frequency and as a result of this significant *RAO* values over a large part of the normal wave frequency range. Almost all wave energy will be transferred into heave motions, which results in a large motion spectrum. An extreme example is the wave buoy, which has (ideally) an *RAO* of 1.0 over the whole frequency range. Then the response spectrum becomes identical to the wave spectrum, which is of course the aim of this measuring tool. It should follow the water surface like a sea gull!
- The ship, with a lower natural frequency, transfers a smaller but still considerable part of the wave energy into heave motions.
- The semi-submersible however, with a very low natural frequency (large mass and small intersection with the water line), transfers only a very small part of the wave energy; very low first order heave motions will appear; it remains essentially stable in the waves.

One can conclude that the natural frequency is a very important phenomenon which dictates (to a significant extent) the behavior of the structure in waves. Whenever possible, the natural frequency should be shifted out of the wave frequency region.

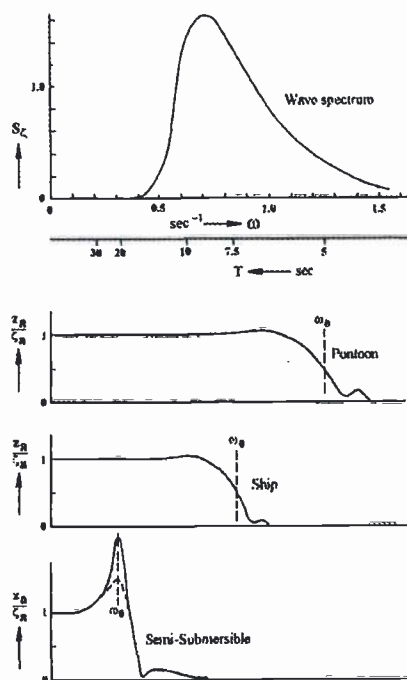


Figure 5.16: Effect of Natural Period on Heave Motions

5.2.2 Second Order Motions

The effects of second order wave forces are most apparent in the behavior of anchored or moored floating structures. In contrast to what has been handled above, these are horizontally restrained by some form of mooring system. Analyses of the horizontal motions of moored or anchored floating structures in a seaway show that the responses of the structure on the irregular waves includes of three important components:

1. A mean displacement of the structure, resulting from a constant load component. Obvious sources of these loads are current and wind. In addition to these, there is also a so-called **mean wave drift force**. This drift force is caused by non-linear (second order) wave potential effects. Together with the mooring system, these loads determine the new equilibrium position - possibly both a translation and (influenced by the mooring system) a yaw angle - of the structure in the earth-bound coordinate system. This yaw is of importance for the determination of the wave attack angle.
2. An oscillating displacement of the structure at frequencies corresponding to those of the waves; the wave-frequency region.

These are linear motions with a harmonic character, caused by the **first order wave loads**. The principle of this has been presented above for the vertically oscillating cylinder. The time-averaged value of this wave load and the resulting motion component are zero.

3. An oscillating displacement of the structure at frequencies which are much lower than those of the irregular waves; the low-frequency region.

These motions are caused by non-linear elements in the wave loads, the **low-frequency wave drift forces**, in combination with spring characteristics of the mooring system. Generally, a moored ship has a low natural frequency in its horizontal modes of motion as well as very little damping at such frequencies. Very large motion amplitudes

can then result at resonance so that a major part of the ship's dynamic displacement (and resulting loads in the mooring system) can be caused by these low-frequency excitations.

[Maruo, 1960] showed for the two-dimensional case of an infinitely long cylinder floating in regular waves with its axis perpendicular to the wave direction that the mean wave drift force per unit length satisfies:

$$\bar{F}' = \frac{1}{2} \rho g \cdot \zeta_{ar}^2 \quad (5.28)$$

in which ζ_{ar} is the amplitude of the wave reflected and scattered by the body in a direction opposite to the incident wave.

Generally only a part of the incident regular wave will be reflected; the rest will be transmitted underneath the floating body. Besides the reflected wave, additional waves are generated by the heave, pitch and roll motions of the vessel. The reflected and scattered waves have the same frequency as the incoming wave, so that the sum of these components still has the same frequency as the incoming wave. Their amplitudes will depend on the amplitudes and relative phases of the reflected and scattered wave components. The amplitudes of these components and their phase differences depend on the frequency of the incident wave, while the amplitudes can be assumed to be linearly proportional to the amplitude of the incident wave. This is because it is the incident wave amplitude which causes the body to move in the first place. In equation form: $\zeta_{ar} = R(\omega) \cdot \zeta_a$ in which $R(\omega)$ is a reflection coefficient. This means that the mean wave drift force in regular waves per meter length of the cylinder can be written as:

$$F'_d = \frac{1}{2} \rho g \cdot \{R(\omega) \cdot \zeta_a\}^2 \quad (5.29)$$

This expression indicates that the mean wave drift force is proportional to the incident wave amplitude squared.

[Hsu and Blenkarn, 1970] and [Remery and Hermans, 1971] studied the phenomenon of the mean and slowly varying wave drift forces in a random sea from the results of model tests with a rectangular barge with breadth B . It was moored in irregular head waves to a fixed point by means of a bow hawser. The wave amplitudes provide information about the slowly varying wave envelope of an irregular wave train. The wave envelope is an imaginary curve joining successive wave crests (or troughs); the entire water surface motion takes place with the area enclosed by these two curves.

A very simple explanation of the low-frequency behavior is based on individual waves in an irregular wave train. Assume that the irregular wave train is made up of a sequence of single waves of which the wave amplitude is characterized by the height of a wave crest or the depth of a wave trough, ζ_{ai} , while the period, T_i , (or really half its value) is determined by the two adjacent zero crossings (see figure 5.17).

Each of the so obtained single waves (one for every crest or trough) is considered to be one out of a regular wave train, which exerts (in this case) a surge drift force on the barge:

$$F_i = \frac{1}{2} \rho g \cdot \{R(\omega_i) \cdot \zeta_{ai}\}^2 \cdot B \quad \text{with: } \omega_i = \frac{2\pi}{T_i} \quad (5.30)$$

When this is done for all wave crests and troughs in a wave train, points on a curve representing a slowly-varying wave drift force, $F'(t)$, will be obtained. This drift force

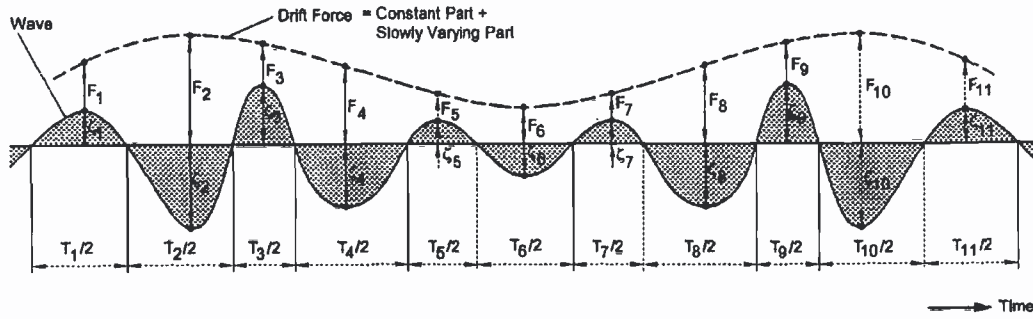


Figure 5.17: Wave Drift Forces Obtained from a Wave Record

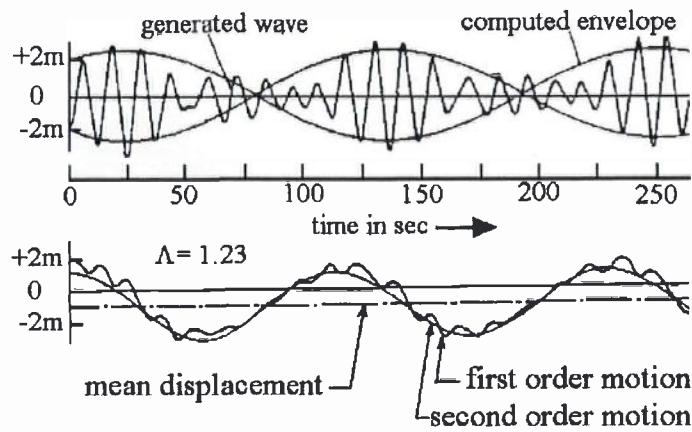


Figure 5.18: Low-Frequency Surge Motions of a Barge

consists of a slowly varying force (the low-frequency wave drift force) around a mean value (the mean wave drift force); see figure 5.17.

These low-frequency wave drift forces on the barge will induce low-frequency surge motions with periods of for instance over 100 seconds. An example is given in figure 5.18. The period ratio, $\Lambda = 1.23$, in this figure is the ratio between the natural surge period of the system (ship plus mooring) and the wave envelope or wave group period. As can be seen in this figure the first order (wave-frequency) surge motions are relatively small, when compared with the second order (low-frequency) motions. This becomes especially true near resonance; $\Lambda \rightarrow 1.0$.

Thus, resonance may occur when wave groups are present with a period in the vicinity of the natural period of the mooring system. Due to the low natural frequency for surge of the bow hawser - barge system and the low damping at this frequency, large surge motions can result. According to [Remery and Hermans, 1971], severe horizontal motions can be built up within a time duration of only a few consecutive wave groups. Obviously, information about the occurrence of wave groups will be needed to predict this response. This is a question for oceanographers.

Bibliography

- [Holtrop, 1977] Holtrop, J. (1977). A Statistical Analysis of Performance Results. *International Shipbuilding Progress*, 24.
- [Holtrop, 1984] Holtrop, J. (1984). A Statistical Reanalysis of Resistance and Propulsion data. *International Shipbuilding Progress*, 31.
- [Holtrop and Mennen, 1982] Holtrop, J. and Mennen, G. (1982). An Approximate Power Prediction Method. *International Shipbuilding Progress*, 89.
- [Hooft, 1970] Hooft, J. P. (1970). *Aspects of Semi-Submersible Platforms*, MARIN publication 400. PhD thesis, Delft University of Technology, The Netherlands.
- [Hsu and Blenkarn, 1970] Hsu, F. H. and Blenkarn, K. A. (1970). Analysis of peak mooring forces caused by slow vessel drift oscillations in random seas. In *Offshore Technology Conference*, number 1159, Houston, USA.
- [Journée and Massie, 1998] Journée, J. M. J. and Massie, W. W. (1998). Offshore Hydro-mechanics (Preliminary Edition). In *Lecture Notes OT4620*, Delft.
- [Maruo, 1960] Maruo, H. (1960). The Drift of a Body Floating in Waves. *Journal of Ship Research*, 4(3).
- [Remery and Hermans, 1971] Remery, G. F. M. and Hermans, J. A. (1971). The slow drift oscillations of a moored object in random seas. In *Offshore Technology Conference*, number OTC 1500, Houston, USA.
- [St. Denis and Pierson, 1953] St. Denis, M. and Pierson, W. J. (1953). On the Motion of Ships in Confused Seas. *Transactions SNAME*, 61:1-53.